NASA Technical Paper 1645

Status of Linear Boundary-Layer Stability Theory and the e^n Method, With Emphasis on Swept-Wing Applications

Jerry N. Hefner and Dennis M. Bushnell

APRIL 1980

NASA

NASA Technical Paper 1645

Status of Linear Boundary-Layer Stability Theory and the e^n Method, With Emphasis on Swept-Wing Applications

Jerry N. Hefner and Dennis M. Bushnell
Langley Research Center
Hampton, Virginia

National Aeronautics
and Space Administration

**Scientific and Technical
Information Office**

1980

SUMMARY

The state of the art for the application of linear stability theory and the e^n method for transition prediction and laminar-flow-control design are summarized, with new analyses of previously published low-disturbance, swept-wing data presented. The major difficulty was found to be the paucity of detailed information regarding stream and wall disturbances and their receptivity within the boundary layer. For any set of transition data with similar stream disturbance levels and spectra, the e^n method for estimating the beginning of transition worked reasonably well; however, even within a given data set, the value of n could vary significantly, evidently depending upon variations in disturbance field or receptivity. For data where disturbance levels were high, the values of n were appreciably below the usual average value of 9 to 10 obtained for relatively low disturbance levels. It is recommended that the design of laminar-flow-control systems be based on conservative estimates of n and that, in considering the values of n obtained from different analytical approaches or investigations, the designer explore the various assumptions which entered into the analyses.

INTRODUCTION

The continuing and deepening shortage of natural petroleum resources has placed increased emphasis upon viscous drag reduction. For conventional take-off and landing (CTOL) transport aircraft, turbulent skin-friction drag is typically on the order of 50 percent of the total cruise drag (ref. 1), and the fraction is much larger for many hydrodynamic applications. For vehicles (or portions thereof) having moderate Reynolds number (100×10^6 or less), application of laminar flow control (LFC) could provide significant increases in fuel efficiency (ref. 2). (See fig. 1.) For attached flows, LFC can be obtained by one or a combination of methods including the following: suction, heating in water, cooling in air (Mack's first mode disturbances), favorable pressure gradient (in two-dimensional or axisymmetric flows), and convex curvature. Several of these approaches have experimentally yielded laminar flow in the Reynolds number range of 50×10^6 (e.g., ref. 3). This range of Reynolds number is approximately an order of magnitude greater than the "uncontrolled" transition location and is sufficient to be of interest in such applications as aircraft wings and some submersibles.

The purpose of the present paper is to summarize, from an engineering point of view, the state of the art of linear stability theory and the e^n method for the prediction of boundary-layer transition and LFC design on swept wings. The following quote from reference 4 interjects the proper perspective regarding the use of linear stability theory for estimating boundary-layer transition:

> At any speeds, the rational approach to prediction of transition probabilities depends strongly on the relative roles of

> the linear and nonlinear processes leading to transition. If, for a given design, the linear [process] . . . should correspond to a major portion of the roads to turbulence, then stability theories would provide us with an invaluable tool. Should there be some bypass of the theoretical models . . . these must be fully charted, experimentally (and/or theoretically with accurate non-linear theory) before the linear tool can be used in its, thus circumscribed, domain of applicability.

In the present work, the relationship between linear stability theory and transition will be reviewed and then the LFC application will be discussed. Using linear stability theory and the e^n method, new analyses of some existing limited swept-wing data will be presented and discussed.

SYMBOLS

A	amplitude of boundary-layer disturbance
A_o	amplitude of boundary-layer disturbance at point of neutral stability
C_L	lift coefficient
C_p	static pressure coefficient
$C_{q,o}$	suction rate coefficient, $-(\rho v)_o/\rho_\infty u_\infty$
c	wing chord measured parallel to free-stream direction
f	disturbance frequency
M	Mach number
n	logarithmic exponent of integrated amplitude (amplification) ratio, $e^n = A/A_o$
p'	fluctuating static pressure
R_c	free-stream Reynolds number based on wing chord
R_x	free-stream Reynolds number based on distance in chordwise direction
R_θ	free-stream Reynolds number based on momentum thickness
ΔT	surface overheat temperature difference
u	velocity parallel to free-stream direction
u'	mean fluctuating velocity in free-stream direction
v	suction velocity normal to surface

x	distance measured in chordwise direction
x_o	distance at point of neutral stability
y	distance normal to chord
α	angle of attack
β	Falkner-Skan pressure gradient parameter
δ^*	boundary-layer displacement thickness
θ	boundary-layer momentum thickness
Λ	leading-edge wing sweep angle
λ	disturbance wavelength
λ_θ	pressure gradient parameter, $\frac{\theta^2}{\mu}\frac{du}{dx}$
μ	viscosity
ρ	density
ψ	angle of line normal to disturbance wavefront and measured relative to free-stream direction
ω_i	nondimensional disturbance amplification (growth rate)

Subscripts:

crit	position above which disturbances become unstable
max	maximum
o	wall
T	beginning of transition
∞	free stream

APPLICATION OF STABILITY THEORY TO TRANSITION

PREDICTION FOR TWO-DIMENSIONAL FLOWS

Transition Process

Several excellent reviews have summarized the relationship between stability theory, transition, and the known physical processes occurring in the

transition region for the two-dimensional, zero-pressure-gradient case (e.g., refs. 5 to 13). This transition process is indicated schematically in figure 2. (See also fig. 1 of ref. 11.) Stream and wall disturbances are somehow internalized by the boundary layer (i.e., Morkovin's "receptivity" problem) and then selectively amplified by the viscous flow. Depending upon the nature and level of the disturbances, this amplification can be either linear or nonlinear. The four most important elements in the transition process are (1) the stream and wall disturbance environment (". . . transition occurs because of disturbances and not just as a result of an unstable boundary layer" (ref. 14)), (2) the receptivity of these disturbances, (3) their subsequent growth, and (4) breakdown into wall "turbulence." Conventional stability theory treats only a portion of one of these elements (i.e., item (3)), and for linear theory to be applicable, items (1) and (2) must result in relatively weak disturbances.

Application of Stability Theory

The major problem in the application of stability theory to the prediction of transition is the extreme lack of detailed knowledge concerning stream and wall disturbances and the receptivity process. The mean viscous-flow development, required as input to stability theory, can now be calculated (using numerical methods and digital computers) for quite general cases. Also, the stability theory itself has now been generalized to include three-dimensional (ref. 15) and nonparallel effects (refs. 16, 17, and 18). Experiments indicate that nonlinear effects originate at amplified disturbance levels on the order of 0.5 to 1 percent, and if the initial (internalized) disturbance levels in the viscous flow are unknown, then one does not know how much or over what distance the linear disturbances amplify before becoming nonlinear.

Approaches to the problem of relating stability theory to transition include the Reynolds stress method of Liepmann (ref. 19), the well-known e^n method (refs. 20 and 21), and the modified e^n and amplitude methods of Mack (refs. 6, 14, and 22). The e^n method is the only one of these methods which does not directly require a knowledge of the initial disturbance amplitude level. However, the actual n value does depend upon the free-stream disturbance level, as shown, for example, by Mack (ref. 14). Also, as has been noted many times, the e^n method generally gives correct trends for the influence of various mean profile modifications on the disturbance growth (e.g., wall suction/cooling, pressure gradient, etc.).

The e^n method, where

$$n = \log (A/A_O) = \int_{x_O}^{x_T} (\text{linear amplification rate})\, dx$$

for the most amplified disturbance frequency, works fairly well for a given set of two-dimensional data, but typically n for transition varies between data sets, becoming smaller and more uncertain as the background disturbance level increases.

There are at least three distinguishable types of two-dimensional/axisymmetric experiments which tend to group the n values for transition. At the upper end, with n values of 0(15), are sailplanes (ref. 23); here the disturbance field is extremely low (i.e., no propulsion sound field and low unit Reynolds number with corresponding decreased roughness sensitivity). The middle group, the famous e^9 data (refs. 20, 21, and 24 to 26), comes from more usual flight experiments where some propulsion noise is present and the unit Reynolds number is higher; other disturbances such as insects, surface irregularities, ice clouds, and dust, however, are still "subcritical." Also included in this e^9 data are results from low disturbance ($u' \cong 0(0.05$ percent)) laboratory facilities. The third set of data (e.g., fig. 7 of ref. 20) is centered about $n = 5$ and comprises results from "conventional" ($u' \cong 0(0.5 \rightarrow 1$ percent)) facilities. For even larger disturbances such as seen by turbine blades and propeller wake regions, the n values may even approach zero or transition can occur "subcritical." It should be noted that the most important disturbance level is the disturbance energy near the critical frequency. A large rms fluctuating level may, in fact, have low amplitude critical levels, depending upon the spectra. The consensus as to why the e^n method seems to correlate a given set of data is that for a relatively low disturbance level at the most amplified frequencies, most of the amplification is, in fact, linear; the nonlinear portion is relatively short. (See refs. 10 and 11 and fig. 3.)

The obvious result from this discussion is that the e^n method is only as good (for data extrapolation) as our knowledge of the particular disturbance field involved. As Mack states in reference 6, ". . . any transition criterion of an empirical nature can only be valid for a very specific disturbance environment." There are two additional cautions on the e^n method. First, a value such as nine for transition represents the average of a number of data points and must be treated as such for design. In the e^9 "data set," individual n values can vary appreciably, even for the same flight or facility and on the same model from day to day. Therefore, a design must be based upon a conservative approach (e.g., $n \cong 7$) once the disturbance field, receptivity, and mean flow details are known to be within the purview of the e^9 data set. The second caution concerns the direct comparison of n values from one calculation/investigation with those from another. The final n value for specific transition data is a function of the various assumptions which entered into the calculation (i.e., whether the mean flow was assumed similar (typical of earlier work) or nonsimilar, whether nonparallel effects were included in the stability theory and, if included, which particular terms were actually used). An additional possible source of discrepancy is whether spatial or temporal theory is employed. If temporal theory is used, then some velocity, generally the group velocity, is required to convert the results to the spatial case. In some of the older work, the phase speed was used rather than group velocity.

The results of figure 4 (taken partially from fig. 5 of ref. 27) illustrate the difficulty that can arise from using stability results without evaluating the underlying assumptions that went into the analyses. The transition data shown were obtained in flight on the two-dimensional, unswept airfoil of the "Snark" airplane (ref. 28). Superficially, the figure indicates that the e^9 method grossly underpredicts the transition data in adverse pressure gradients. Unfortunately, a "similar" boundary-layer analysis was used in reference 27 to evaluate the validity of the e^9 method; in fact, the e^9 curve shown was

taken directly from reference 20, which developed curves for exactly "similar" adverse pressure gradient flows on two-dimensional wedge-type geometries (constant λ flows). The boundary-layer flow on the Snark airfoil was "nonsimilar;" R_θ built up in the forward, favorable pressure gradient (stable) region, with the actual extent of large adverse pressure gradient being quite limited. (See fig. 21 of ref. 28.) Using a current nonsimilar analysis to evaluate the e^9 method yields a significantly more accurate prediction of the Snark data and a contradictory conclusion regarding the applicability of the e^9 method to adverse pressure gradient flows. For the case where $\lambda_{\theta,T} \cong -0.06$ ($R_C = 3 \times 10^6$, $C_L = 1.07$, and $R_{\theta,T} \cong 780$), the nonsimilar analysis using the e^9 method predicted $R_{\theta,T} \cong 680$, whereas the similar analysis predicted $R_{\theta,T} \cong 135$; for e^{13}, the nonsimilar analysis predicted $R_{\theta,T} \cong 780$. This example should serve as a caution against indiscriminate use of "magic plots" such as figure 5 (taken from ref. 29); each case should be individually studied by using advanced tools such as the Sally (ref. 15) or TAPS (ref. 30) computer codes.

DISTURBANCES, RECEPTIVITY, AND APPLICATION OF STABILITY THEORY TO LAMINAR FLOW CONTROL

There is a fundamental difference in philosophy between using stability theory for prediction of transition location and for design of optimized LFC systems. In the LFC case the flow can, and indeed must, be kept in the linear range. Once flow fluctuations have amplified into the nonlinear range, most of the LFC devices (suction, heating/cooling, etc.) lose much of their efficiency. For example, less overall suction is used if disturbances are kept small, rather than letting them grow fairly large and then reducing their amplitude with increased amounts of suction.[1] This discussion presupposes knowledge of the fact that, in an LFC system, it is usually extremely inefficient to keep the flow stable. Some growth must be allowed to obtain maximum benefit; however, the question is how much growth (as computed by stability theory) should be allowed. In contrast to this "linearized" LFC case, the conventional transition prediction scenario involves at least some nonlinear growth, as the flow eventually undergoes transition.

The application of stability theory to the LFC problem would appear to be straightforward. In order to avoid the nonlinear growth region, one selects a design criterion at least an order of magnitude lower than conventional transition criteria. (See fig. 3.) For the e^9 data set, which for two-dimensional flows should probably be e^7 to account for inherent uncertainty (data scatter caused at least partly by variations in background disturbances and receptivity), one should "back off" to approximately e^5 to ensure linear growth. The possible problem with even this conservative number is still the level, spectra, and nature of background and internalized disturbances. Having previously established the first-order importance of stream and wall disturbances (and

---

[1]This information was obtained in a private communication with Werner Pfenninger, The George Washington University Joint Institute for Advancement of Flight Sciences at NASA Langley Research Center, Hampton, Virginia.

their receptivity) on the application of stability theory to LFC, the types of disturbances which must be considered in LFC design will be briefly examined.

Disturbance Environment

The following list illustrates the many possible stream and wall disturbances that are important in LFC applications. Note, however, that stability theory is not applicable when these disturbances are supercritical (i.e., when they are sufficiently large to promote instantaneous boundary-layer transition). Typical references discussing each of these indicated problem areas (i.e., refs. 31 to 67) are also provided.

I. Roughness (refs. 36, 42, 49, and 61 to 64)
- Insect remains
- Discrete
- Continuous
- Two dimensional
- Three dimensional
- Steps
- Gaps
- Particle impact/erosion
- Corrosion
- Leakage

II. Wall Waviness (refs. 55, 59, and 67)
- Two dimensional
- Three dimensional
- Single wave
- Multiple wave
- Distortion under load
  - Aerodynamic
  - Hydrodynamic
  - Sun/heat

III. Surface and Duct Vibration (refs. 33 and 58)

IV. Acoustic Environment (refs. 21, 37, 40, 41, 43, 48, 51, and 59)
- Attached flow
- Separated flow
- Propulsion system
- Vortex shedding

V. Stream Fluctuations and Vorticity (refs. 13, 41, 42, 44 to 47, 50, 52 to 54, 56, 57, and 59)
- Propeller wakes
- Ocean surface
- Body wakes
  - Fish
  - Aircraft
- High shear areas
  - Weather fronts

Jet stream edges
Ocean currents

VI. Particles (refs. 32, 65, and 66)
Ice clouds
Rain
Algae
Suspensions

VII. LFC-Systems Generated Disturbances (refs. 31, 34, 35, 38, 39, 59, and 60)
Vortex shedding (blocked slots, holes, pores)
Acoustic or chugging
Pore disturbances
Nonuniformities

Although the length and complexity of the previous list of "spoilers" for the e^n method (or any stability theory approach) is alarming, an even more serious problem arises from the fact that the influence or relative dominance of any of these disturbances is a function of (1) wavelength, frequency, wave orientation, and amplitude of that disturbance (also whether linear or nonlinear), (2) the simultaneous presence and nature (spectra, amplitude) of other disturbance types (these do not generally appear alone but in combinations of various strengths and the number of possible combinations is obviously quite large), and (3) the history of the mean viscous flow as it is influenced by the usual modifiers such as surface curvature, pressure gradient, surface mass transfer, wall temperature, and unit Reynolds number.

Except for a few restricted instances (see, for example, ref. 8), these disturbances are not yet directly included into stability theories, and their forced normal-mode solutions are not yet available. Hence, one is reduced to the uncomfortable state of having to experimentally examine the tolerance of one's scaled mean-flow history to each of the applicable disturbance sources. (Note that the specific areas of concern are of course dependent upon the actual LFC application mission.) This procedure can be quite expensive since the requisite tests must be conducted with extreme care in special facilities and is made even more questionable by (1) the possible further destabilization of disturbance mode combinations, (2) our relative ignorance concerning actual disturbance levels in flight, and (3) the ever present possiblity of "new problems" (ref. 11) such as the spanwise contamination problem encountered in flight on the X-21 (ref. 59).

To finish this section on a more optimistic note, much of the actual flight and open ocean experience with various types of LFC has been more favorable than the ground facilities tests would indicate. (Recall that this has already been indicated in the previous discussions of the effects of disturbances on n values for the e^n method.) Note the following quote (circa 1940) on flight results obtained on unswept wings with extended regions of laminar flow (ref. 68): "These (flight) tests have demonstrated that marked turbulence effects exist even in the (NACA) low turbulence tunnel (in early configuration, not down to "final" u' level), with the result that the drag increase with Reynolds number is shown by all wind tunnel tests to occur at much too low a

Reynolds number. The practical result is that the airfoils now appear useable at a Reynolds number of the order of twice that previously thought to limit their usefulness." Another interesting example comes from the X-21 program. Figure 6 (taken from ref. 69) indicates that considerably higher noise levels (approximately 5 to 7 dB higher) could be tolerated in flight than in wind-tunnel experiments. This may be at least partially due to the relative absence of small-scale stream vorticity fluctuations in the flight situation (a possible example in the wind tunnel of degradation of criteria due to presence of multiple disturbance modes). As a final example, the following quote is taken from the abstract of a Soviet paper documenting an LFC flight suction experiment (ref. 70) on a remotely piloted vehicle with a two-dimensional airfoil:

> Due to smallness of the disturbances acting in free flight as compared with a wind tunnel, the laminar part of the boundary layer is larger . . . . Hence the use of suction in free flight requires a smaller suction rate for obtaining the same size of the laminar zone.

Laminar Flow Control on Swept Wings

As an illustrative example of the application of stability theory to LFC, consider the transonic swept-wing case, which is of current interest to the LFC element of the NASA ACEE program (ref. 71). Compared to the straight wing, the swept-wing situation has two additional problems, both due to the three-dimensional nature of the mean flow. The first problem, originally defined by Owen and Randall (ref. 72), involves formation of stationary, approximately streamwise disturbance vortices in the regions of both adverse and favorable presssure gradient. These vortices are predictable by three-dimensional stability theory and, fortunately, are relatively easily stabilized by suction (ref. 59). They occur because of inflection points in the boundary-layer cross-flow velocity profiles. The second problem on the swept wing is the possibility of spanwise contamination along the leading edge, from either the turbulent fuselage boundary layer or large disturbances in the leading-edge region. When examining swept-wing transition data, it should first be determined whether this spanwise contamination problem is present; otherwise, the inferred n values could be quite low and erroneously interpreted. Several techniques exist for dealing with this spanwise contamination problem (ref. 59).

Although amenable to control by suction, the swept leading-edge cross-flow region generally requires considerably more suction for LFC than the two-dimensional situation at the same Reynolds number. The work of Srokowski and Orszag (ref. 15) has shown that an e^n type method could be applied to the swept-wing case. In the present paper, the e^n approach for swept wings will be examined using a larger data set than examined in reference 15. Most of the available low-disturbance swept-wing transition data is sumarized in table I (refs. 73 to 98) and includes wind-tunnel and flight data. The Cranfield data (entry 1), the 33° Northrop wing (entry 6), and the Michigan test (entry 4) have not previously been analyzed by the e^n method. Entries 2 and 3 were examined in reference 15; entry 3 was also studied in reference 23.

The application of the e^n method for two-dimensional cases is relatively straightforward. The integration is carried out in the downstream direction and the frequency is fixed. This constitutes a well-posed stability problem. However, the three-dimensional case is another matter, with several fundamental difficulties. The first difficulty occurs because there are now three rather than two variables (λ, f, and ψ, rather than just λ and f) and thus the direction which should be used to integrate the disturbance growth for application of the e^n method is uncertain. This problem arises because stability theory is not a solution to the initial value problem. Various approaches to overcoming these problems have been used. Reference 15 advocated the "envelope" method, where the frequency is fixed and the orientation and wavelength are simultaneously optimized to give the maximum local growth at that frequency. Several frequencies are examined until a global maximum is found, with spatial integration occurring in the direction of the real part of the group velocity. The Sally code of reference 15 has since been modified to include other options such as "fixed wavelength and frequency" and "fixed orientation and frequency." Other approaches include integrating in the direction of the local potential flow (refs. 23 and 99) and solution of a kinematic wave packet equation (ref. 100). Recently, Nayfeh (ref. 101) has derived the propagation condition that $d\alpha/d\beta$ must be real (here α and β are defined as the wave number components in the streamwise and spanwise directions, respectively). Private communications with S. G. Lekoudis at Lockheed-Georgia Company and with A. Nayfeh of Virginia Polytechnic Institute and State University indicate that the results using the Nayfeh expression are quite similar to the envelope method (ref. 15).

The second difficulty associated with applying the e^n method to swept wings concerns the variegated nature of the disturbance development over the airfoil. Modern "supercritical" type airfoils and, to a lesser extent, older airfoil designs, have a region of relatively small pressure gradient in the midchord region on the upper surface. This acts as a Tollmien-Schlichting (T-S) disturbance growth region which separates cross-flow regions (with different cross-flow directions) in the front and rear portion of the airfoil. The assumption made in reference 15 was that disturbances generated in the forward, cross-flow dominated region (for Λ large) do not influence the T-S growth, and, in turn, the T-S waves do not affect the cross-flow disturbance growth in the rearward region. This simplification is probably acceptable except for two cases: (1) where the "upstream" disturbances grow large enough to exert a nonlinear, profile-modifying influence and (2) for the transonic case, where the T-S waves have an oblique orientation. This latter possibility should be checked, but no suitable transonic swept-wing transition data are yet available (except perhaps for the X-21 data) due to the large disturbance levels, both vortical and acoustic, which exist in conventional transonic tunnels. NASA Langley Research Center is currently involved in an effort to develop and conduct transition tests in a low-disturbance transonic tunnel.

APPLICATION OF e^n METHOD TO LOW-DISTURBANCE SWEPT-WING DATA

Although the e^n method has severe limitations due to current unknown factors such as free-stream disturbances and their receptivity within the boundary layer, the question remains as to whether the e^n method can be used as a design tool for estimating transition and hence suction rates, and distributions

for laminar flow control in the cross-flow region on swept, tapered airfoils. This section will explore results obtained using an advanced version of the Sally stability theory code (ref. 15) to analyze the integrated amplification ratios (i.e., "n" factors) for four sets of low-disturbance, swept-wing data. The advanced Sally code included improvements to make the code user oriented and versatile: 40 percent less memory, 45 percent less run times, and additional options for calculating local disturbance growth rates. Results obtained using two of the local growth rate options (i.e., the envelope method and the fixed wavelength/frequency method) will be presented and discussed. (See ref. 15 for a discussion of these methods.) In addition to the previous results of reference 15, the data analyzed herein will include two sets of flight data, one without suction and the other with suction (entries 1 and 7 in table I), and two sets of wind-tunnel data, both with suction (entries 4 and 6 in table I). Full-chord laminar flow was obtained in each of the suction data sets; hence, the intent of the present analyses is to compare the calculated n values for these data with those determined for data without suction where transition occurred (i.e., the Cranfield data (ref. 76) and the Ames data (ref. 85)). Results of the present analyses are summarized in table II.

Cranfield Data

Transition data were analyzed for eight flights (u_∞ = 46.3 to 56.7 m/sec) of a large, untapered, untwisted, unsucked 45° swept half wing mounted as a dorsal fin upon the mid-upper fuselage of an Avro Lancaster airplane (refs. 73 to 76). The airfoil section was made up of two semiellipses, one of which constituted a faired or foreshortened trailing edge and the other corresponding to the leading-edge portion of a 10-percent-thick airfoil with "effective" chord of 3.3 m measured in the free-stream direction. A sketch of the wing section with the measured pressure distribution for the cases analyzed is presented in figure 7. Calculations were performed to the estimated beginning of transition. Since the transition data in reference 76 represented the end of transition, it was necessary to estimate where the beginning of transition occurred for comparison with the stability analyses. Using the limited surface pitot pressure distributions given in reference 76 to indicate how transition was defined, the ratio of the beginning of transition to the end of transition x_{BT}/x_{ET} was determined to be $x_{BT}/x_{ET} \approx 0.54$ and is used in the present analysis.

The integrated cross-flow instability amplification ratios obtained from both the envelope method and the fixed wavelength/frequency method for the cases analyzed are presented in figures 8 and 9, respectively. Table II summarizes the maximum n factors obtained for these Cranfield data, as well as those found in reference 15 for the Ames swept-wing wind-tunnel data. The major result from the present analysis of the Cranfield data is that although the n factors vary significantly from 7.6 to 11 for the envelope method and from 6.1 to 9.2 for the fixed wavelength/frequency method, they are completely consistent with those obtained in reference 15 for the Ames data. The average of the n values for the Cranfield data using the envelope and fixed wavelength/frequency approaches are 9.7 and 7.2, respectively; for the Ames data, they were 10.1 and 6.9, respectively. The average of both the Cranfield flight and Ames wind-tunnel data is 9.8 for the envelope method and 7.2 for the fixed wavelength/frequency method. This result suggests that the background disturbance levels

in the very best low-disturbance wind-tunnel experiments may not be all that different from those found in moderately good flight experiments even though the sources of the background disturbances are quite different (at low speed).

Another interesting result of the present calculations is shown in figure 10. In contrast to the results of reference 15 where the most amplified cross-flow instabilities occurred at frequencies very near or equal to zero, the most spatially amplified instabilities found for the Cranfield data occurred at significantly higher frequencies for both the envelope and fixed wavelength/frequency methods. Therefore, caution is advised when trying to find the most unstable frequency; the most unstable frequency should not be assumed a priori to be zero but is a function of the mean boundary-layer profile and how it was developed.

Typical stability characteristics obtained with the envelope and fixed wavelength/frequency analyses are shown in figures 11 and 12 for the case of $\alpha = 2^{\circ}$ and $R_c = 9.5 \times 10^6$. As expected for both analyses, the local disturbance amplification rate ω_i grows to a maximum in the wing leading-edge region and then decreases. Another interesting result for the envelope method is that the most amplified wavelength λ/c for each chordwise position changes by a factor of 3 even though the cross-flow wave-orientation angle relative to the free-stream direction ψ changes very little. In contrast, for the fixed wavelength/frequency method, the wave angle ψ changes significantly from approximately 77° at the leading edge to 86° at transition. The variation in disturbance wave angle could possibly be used as a discriminator in an experiment to sort out the actual physical-growth processes.

Northrop X-21 Data

Figure 13 presents a typical pressure distribution and equivalent area suction distribution representative of a Northrop X-21 flight case (refs. 95 to 97), where full-chord laminar flow was obtained for $R_c = 22.5 \times 10^6$ at a Mach number of 0.8 and a lift coefficient of 0.3. Integrated disturbance amplification ratios obtained using both the envelope and fixed wavelength/frequency analyses of these data are shown in figures 14 and 15; also shown is the sensitivity of the n factors to suction level. Note that $C_{q,o}$ represents the "quoted" minimum flight suction level and distribution as shown in figure 13(b); the suction values of $0.85C_{q,o}$ and $0.70C_{q,o}$ have the same distribution as $C_{q,o}$ but have levels that are reduced by 15 and 30 percent, respectively. Another important point that should be noted prior to discussing the analysis of these transonic data is that compressibility is not included in the present stability calculations, and hence, integrated amplification rates obtained for the trailing-edge regions could be too large by approximately 14 to 40 percent; Mack (ref. 100) has shown compressibility to be important in determining the values of n for the trailing-edge cross-flow region of transonic airfoils. The e^n method of analysis herein is being used as a diagnostic tool to examine the X-21 data to see if anything unusual may have occurred since these data represent the only swept-wing transonic data available.

Examination of figures 14 and 15 for the quoted flight suction distribution reveals that the integrated amplification ratios on the X-21 airfoils are sub-

stantially lower for both stability analyses than those previously found for either the unsucked Ames wind-tunnel data (i.e., ref. 15 and table II) or the unsucked Cranfield flight data. For the envelope method, the maximum n for $x/c < 0.5$ was 0.8 and for $x/c > 0.5$ was 1.5 at a frequency of 250 cycles/sec; the fixed wavelength/frequency method produced a maximum n of 1.5 for $x/c > 0.5$ and found no amplified instability for $x/c < 0.5$ at a frequency of 250 cycles/sec and a wavelength of 0.0015. It can be postulated that such effects as compressibility, radiated boundary-layer noise from the attached flow on the fuselage, vibration, and noise associated with (1) possible unsteady separated flow regions downstream of the canopy, (2) propulsion and suction engines, and (3) slot suction system may have exacerbated the cross-flow stability problem and forced an extensive amount of suction to be used to maintain full-chord laminar flow. This postulation, coupled with the fact that the X-21 local suction levels and distributions were not directly measured, led to an analysis of the growth sensitivity to suction level.

Reducing the level of the suction had a profound influence upon the computed n factors, as seen in figures 14(a) and 15(a), for frequencies and wavelengths that produced maximum integrated amplification ratios at the airfoil trailing edge. A reduction of 15 percent in the level of suction produced an increase in n from 0.8 to 2.6 for $x/c < 0.5$ and from 1.5 to 5.8 for $x/c > 0.5$ using the envelope analysis. An additional 15-percent reduction in suction level increased these n factors to 5.2 for $x/c < 0.5$ and 12.1 for $x/c > 0.5$. Similar behavior was obtained for the fixed wavelength/frequency analysis for $x/c > 0.5$; however, for $x/c < 0.5$, no cross-flow instability was amplified until the suction level was reduced to below 85 percent of the quoted flight value. Although compressibility, vibration, and noise may very well have been severe problems on the X-21 flight, the present analyses show that the integrated amplification ratios are extremely sensitive to level of suction and that small changes in suction can cause large changes in integrated amplification ratios.

Figures 14(b) and 15(b) illustrate the sensitivity of the maximum integrated amplification ratios with frequency. For both the envelope and fixed wavelength/frequency analyses, the sensitivity of the maximum n factor with frequency increases as the suction level is reduced for $x/c > 0.5$; the maximum n factors occur at or near a frequency of zero. However, for $x/c < 0.5$, the maximum n factors are relatively insensitive to frequency changes, particularly for the envelope method. These results reinforce the caution given in the analysis of the Cranfield flight data; that is, when looking for the most amplified frequencies, do not assume a priori the influence of frequency on the maximum integrated amplification ratios.

Ames 33° Swept-Wing Data

In the low-drag, boundary-layer suction experiments (refs. 91 to 95), a 33° swept wing having a 3-m chord and an unsymmetric 15-percent-thick airfoil suction was tested at the NASA Ames 12-Foot Pressure Wind Tunnel. Full-chord laminar flow was obtained up to chord Reynolds numbers of 29.6×10^6 for configurations with chordwise slots in the leading-edge region and spanwise slots downstream of the leading-edge region. Because transition at higher Reynolds

numbers was evidently a result of disturbances originating at the suction slots due to wake-flow oscillations caused by the high slot Reynolds number (greater than 120) in the slots in the adverse pressure gradient region, the current analysis is focused only on the data at lower Reynolds numbers where full-chord laminar flow was obtained at $R_c = 29.6 \times 10^6$. The pressure and suction distributions used in the analysis are shown in figure 16 for a free-stream velocity of 30 m/sec and an angle of attack of 1.5^o. The suction levels for this investigation are approximately equal to those designated "S1" in the analysis of the Ames 30^o swept wing which achieved full-chord laminar flow at $R_c = 23.7 \times 10^6$ (ref. 15).

Figure 17 presents integrated disturbance amplification ratios obtained by the envelope analysis for a stationary cross-flow instability (i.e., $f = o$) and for a frequency of 250 cycles/sec. These frequencies were found to give the most amplified disturbances over the rearward and forward sections of the airfoil, respectively; the stationary cross-flow instability was significantly more amplified over $x/c > 0.5$ than the $f = 250$ cycles/sec instability; however, for $x/c < 0.5$, the higher frequency was the more amplified. The maximum n of 3.5 at the airfoil trailing edge for the current analysis is in very good agreement with that found in reference 15 for the Ames 30^o swept wing with comparable suction levels (e.g., $n \cong 3.9$). It should be noted that these suction levels may have been much larger than necessary.

Figures 18 and 19 show the variation in maximum integrated amplification ratios with frequency for both the envelope and fixed wavelength methods. The trends with frequency for both methods agree with those found for the X-21 data (i.e., the maximum integrated amplification ratios over the rearward adverse pressure gradient are more sensitive to changes in frequency than those over the front half of the airfoil). A more important result, shown in figure 19 for the fixed wavelength/frequency, is that the most amplified wavelengths over the front half of the wing are significantly smaller than those over the rearward half of the airfoil. It is also interesting to note that the maximum n value obtained by the fixed wavelength/frequency method over the rearward portion of the 33^o swept wing ($n = 2.9$) is approximately equal to that found in the analysis of the Ames 30^o swept wing for suction "S1" in reference 15 and that this maximum occurs for a stationary cross-flow instability having a wavelength of approximately 0.0015 in both cases.

Michigan 30^o Swept-Wing Data

Full-chord laminar flow was obtained up to chord Reynolds numbers of 11.8×10^6 in these experiments on a 30^o swept wing having a 2.1-m chord and a symmetric 12-percent-thick airfoil section (modified NACA 66-012 section). Suction was applied through 86 fine slots from 25-percent chord to 95-percent chord. The data analyzed in the current report achieved full-chord laminar flow at $R_c = 10.6 \times 10^6$ for a free-stream velocity of 76 m/sec and angle of attack of 0^o. The pressure and suction distributions used in the present analysis are shown in figure 20. The suction distribution shown is a faired representation so as to avoid discontinuities that would result in computing difficulties.

Figure 21 shows the integrated amplification ratios over the airfoil surface for various frequencies using the envelope method. The important result shown in this figure is the level to which the instabilities grow before becoming damped; n factors between 9.0 and 11.3 were found for frequencies up to 500 cycles/sec. The reason for these large integrated amplification ratios is probably (1) the relatively low levels of suction compared with those used in the X-21 and the Ames 30° and 33° swept-wing cases and (2) the suction being initiated far from the leading edge, which resulted in cross-flow instabilities close to the leading edge being amplified to relatively large levels before suction was applied. The suction levels indicated were the minimum necessary to keep full-chord laminar flow; experimental observations in reference 86 confirm this hypothesis as turbulent bursts were observed relatively far forward on the airfoil at $\alpha = 0^{\circ}$ and $R_c = 10^7$.

Figures 22 and 23 show the sensitivity of the maximum integrated amplification ratios to changes in frequency over the wing surface using the envelope and fixed wavelength/frequency analyses. For both analyses, the maximum n factors occur at frequencies other than the zero-frequency stationary cross-flow mode and are relatively sensitive to changes in frequency except for wavelengths less than 0.001. Maximum n values from the fixed wavelength/frequency analysis (see fig. 23) follow the same trend as those determined by the envelope method and approach the average value of n for transition (n = 9 to 10) as determined in the present analysis of the Cranfield flight and Ames wind-tunnel swept-wing data without suction. (See table II.)

Summary Remarks

One problem area not addressed in the current analyses of the available data is the question of whether the maximum n factors for transition are different for the forward and rearward portions of the swept wing, as suggested in reference 15. Reference 15 concluded from its analysis of the Ames 30° swept wing with suction and full-chord laminar flow that the allowable integrated amplification ratios over the rearward portion of the wing may be lower than those for the forward portion of the wing. This conclusion is not substantiated by the current analysis of the X-21 data and the Ames 33° swept-wing data. For both of these sets of data, the calculated amplification ratios over the rearward portion of the wings were equal to or greater than those obtained over the forward portion of the wing. The difficulty is that there are essentially no low-disturbance data available for swept wings where transition occurred beyond the midchord region; hence, the only information available is for airfoils with suction, and many of these either have full-chord laminar flow or slot disturbances that cause premature transition.

The calibration of the e^n method for cross-flow transition prediction is far from complete. The current analysis has explored the application of the e^n method to some of the very few relatively high quality and detailed swept-wing experiments. Further definitive experiments are a necessity for a meaningful calibration of the method.

CONCLUDING REMARKS

The state of the art for the application of linear stability theory and the e^n method for boundary-layer transition prediction and laminar-flow-control (LFC) design has been summarized, and results of advanced stability analyses of previously published low-disturbance swept-wing data have been presented. A major problem was found to be the paucity of detailed information concerning stream and wall disturbances and their receptivity within the boundary layer. For any particular set of two-dimensional or swept-wing data with similar stream disturbance levels and spectra, the e^n method for estimating the beginning of transition works reasonably well; however, even within a given data set, the value of n may vary significantly, evidently depending upon currently uncontrollable variations in disturbance field or receptivity.

Limited low-disturbance flight and wind-tunnel transition data for swept wings were correlated reasonably well using advanced stability analyses and the e^n method. Average values of n at transition, determined using the envelope and fixed wavelength/frequency analyses, were 9.8 and 7.2, respectively. A major implication from these results is that the background disturbance levels in the very best low-disturbance, low-speed, wind-tunnel experiments may not be significantly different than those found in moderately good, low-speed, flight experiments, even though the sources of the disturbances are quite different.

The calibration of the e^n method for swept-wing, cross-flow transition prediction is far from complete. Very few high quality, low-disturbance, swept-wing experiments have been conducted; further definitive experiments are essential for a meaningful evaluation and calibration of the e^n method. Design of LFC systems should currently be based on conservative estimates of n because of (1) the inherent uncertainty in the available data due to variations in background disturbances and receptivity and (2) the need to maintain disturbance growth rates in the linear growth region for efficient LFC system operation. The selection of n for transition may not be that critical, however, for the LFC design process since, as shown herein, small changes in suction have large effects on disturbance growth.

Langley Research Center
National Aeronautics and Space Administration
Hampton, VA 23665
February 15, 1980

REFERENCES

1. Special Course on Concepts for Drag Reduction. AGARD-R-654, June 1977.

2. Hefner, Jerry N.; and Bushnell, Dennis M.: An Overview of Concepts for Aircraft Drag Reduction. Special Course on Concepts for Drag Reduction, AGARD-R-654, June 1977, pp. 1-1 - 1-30.

3. Bushnell, Dennis M.; and Tuttle, Marie H.: Survey and Bibliography on Attainment of Laminar Flow Control in Air Using Pressure Gradient and Suction. Volume I. NASA RP-1035, 1979.

4. Morkovin, Mark V.: On the Many Faces of Transition. Viscous Drag Reduction, C. Sinclair Wells, ed., Plenum Press, 1969, pp. 1-31.

5. Levchenko, V. Ya.; Volodin, A. G.; and Gaponov, S. A.: Kharanteristini Vstoychivosti Progranichnykh Sloyer (Stability Characteristics of Boundary Layers). Siberian Div., Nauka Press (Novosibirsk), 1975.

6. Mack, Leslie M.: Transition and Laminar Instability. NASA CR-153203, 1977.

7. Tani, Itiro: Boundary Layer Transition. Annual Review of Fluid Mechanics, Volume I, William R. Sears and Milton Van Dyke, eds., Annual Rev., Inc., 1969, pp. 169-196.

8. Reshotko, Eli: Boundary-Layer Stability and Transition. Annual Review of Fluid Mechanics, Volume 8, Milton Van Dyke, Walter G. Vincenti, and J. V. Wehausen, eds., Annual Rev., Inc., 1969, pp. 311-349.

9. Obremski, H. J.; Morkovin, M. V.; and Landahl, M: A Portfolio of Stability Characteristics of Incompressible Boundary Layers. AGARDograph 134, Mar. 1969.

10. Berger, S. A.; and Aroesty, J.: "e^9": Stability Theory and Boundary-Layer Transition. R-1898-ARPA (Contract No. DAHC15-73-C-0181), Rand Corp., Feb. 1977. (Available from DTIC as AD A038 908.)

11. Morkovin, Mark V.: Instability, Transition to Turbulence and Predictability. AGARD-AG-236, July 1978.

12. Kozlov, L. F.; and Babenko, V. V.: Experimental Boundary Layer Studies. NAVSEA Translation No. 1759A, U.S. Navy, Apr. 1979.

13. Struminskii, V. V.: Laminar Flow Stability Problems and the Transition to Turbulent Flow. Fluid Mech. - Soviet Research, vol. 1, no. 2, Mar.-Apr. 1972, pp. 121-134.

14. Mack, Leslie M.: Transition Prediction and Linear Stability Theory. Laminar-Turbulent Transition, AGARD-CP-224, Oct. 1977, pp. 1-1 - 1-22.

15. Srokowski, Andrew J.; and Orszag, Steven A.: Mass Flow Requirements for LFC Wing Design. [Paper] 77-1222, American Inst. Aeronaut. & Astronaut., Aug. 1977.

16. Saric, William S.; and Nayfeh, Ali H.: Non-Parallel Stability of Boundary-Layer Flows. VPI-E-75-5, Virginia Polytech. Inst. & State Univ., Feb. 1975.

17. Wazzan, A. R.; Taghavi, H.; and Keltner, Gerlina: Effect of Boundary-Layer Growth on Stability of Incompressible Flat Plate Boundary Layer With Pressure Gradient. Phys. Fluids, vol. 17, no. 9, Sept. 1974, pp. 1655-1660.

18. Wazzan, Ahmed R.: Spatial Stability of Tollmien-Schlichting Waves. Prog. Aerosp. Sci., vol. 16, no. 2, 1975, pp. 99-127.

19. Liepmann, H. W.: Investigation of Boundary Layer Transition on Concave Walls. NACA WR W-87, 1945. (Formerly NACA ACR 4J28.)

20. Smith, A. M. O.; and Gamberoni, Nathalie: Transition, Pressure Gradient, and Stability Theory. Rep. No. ES 26388, Douglas Aircraft Co., Inc., Aug. 31, 1956. (Also available in IX Congrès International de Mécanique Appliquée, Tome IV, Université de Bruxelles, 1957, pp. 234-244.)

21. Jaffe, N. A.; Okamura, T. T.; and Smith, A. M. O.: Determination of Spatial Amplification Factors and Their Application to Predicting Transition. AIAA J., vol. 8, no. 2, Feb. 1970, pp. 301-308.

22. Mack, Leslie M.: Linear Stability Theory and the Problem of Supersonic Boundary-Layer Transition. AIAA J., vol. 13, no. 3, Mar. 1975, pp. 278-289.

23. Runyan, L. James; and George-Falvy, Dezso: Amplification Factors at Transition on an Unswept Wing in Free Flight and on a Swept Wing in Wind Tunnel. AIAA Paper 79-0267, Jan. 1979.

24. Power, John L.: Drag, Flow Transition, and Laminar Separation on Nine Bodies of Revolution Having Different Forebody Shapes. DTNSRDC-77-0065, U.S. Navy, Dec. 1977. (Available from DTIC as AD A048 274.)

25. Kaups, K.: Transition Prediction on Bodies of Revolution. Rep. No. MDC J6536 (Contract No. N66001-74-C-0020), Douglas Aircraft Co., Apr. 1974. (Available from DTIC as AD 778 045.)

26. Huang, T. T.; and Hannan, D. E.: Pressure Fluctuations in the Regions of Flow Transition. Rep. No. 4723, David W. Taylor Naval Ship Research and Development Center, Dec. 1975. (Available from DTIC as AD A022 935.)

27. Hall, D. J.; and Gibbings, J. C.: Influence of Stream Turbulence and Pressure Gradient Upon Boundary Layer Transition. J. Mech. Eng. Sci., vol. 14, no. 2, Apr. 1972, pp. 134-146.

28. Stephens, A. V.; and Haslam, J. A. G.: Flight Experiments on Boundary Layer Transition in Relation to Profile Drag. R. & M. No. 1800, British A.R.C., 1938.

29. Scotti, R. S.; and Corbett, K. T.: Laminar Body Analysis Heat Plus Suction Stabilized. ONR-CR289-013-1F, U.S. Navy, Dec. 1976. (Available from NTIS as AD A040 396.)

30. Tzou, Kent T. S.: Numerical Assessment of the Computer Codes for Analyzing Boundary Layer Transition on a Heated Axisymmetric Body. Rep. No. DT-7802-6 (Contract N00014-77-C-0005 (P0002)), Dynamics Technology, Inc., Nov. 1978. (Available from DTIC as AD A062 887.)

31. Singh, P.; Sharma, V. P.; and Misra, U. N.: Three Dimensional Fluctuating Flow and Heat Transfer Along a Plate With Suction. Int. J. Heat Mass Transfer, vol. 21, no. 8, Aug. 1978, pp. 1117-1123.

32. Effect of Clouds on LFC Applications. Syst. Eng. Group, Res. & Technol. Div., Wright-Patterson AFB, Dec. 1964. (Available from DTIC as AD 454 476.)

33. Garrelick, J. M.; and Junger, M. C.: The Effect of Structure-Borne Noise in Submarine Hull Plating on Boundary Layer Stability. Rep. ONR CR-289-017-1F, U.S. Navy, Nov. 1977.

34. Gaponov, S. A.: Effect of the Properties of a Porous Coating on Boundary Layer Stability. NASA TM-75235, 1978.

35. Strazisar, A.; and Reshotko, E.: Stability of Heated Laminar Boundary Layers in Water With Nonuniform Surface Temperature. Phys. Fluids, vol. 21, no. 5, May 1978, pp. 727-735.

36. Merkle, Charles L.; Tzou, Kent T. S.; and Kubota, Toshi: An Analytical Study of the Effect of Surface Roughness on Boundary-Layer Stability. DT-7606-4 (Contract N00014-77-C-0005), Dynamics Technol., Inc., Oct. 1977. (Available from DTIC as AD A004 786.)

37. Schlinker, R. H.; Fink, M. R.; and Amiet, R. K.: Vortex Noise From Non-rotating Cylinders and Airfoils. AIAA Paper No. 76-81, Jan. 1976.

38. Pfenninger, W.; Bacon, J.; and Goldsmith, J.: Flow Disturbances Induced by Low-Drag Boundary-Layer Suction Through Slots. Phys. Fluids Suppl., vol. 10, no. 9, pt. II, Sept. 1967, pp. S112-S114.

39. Bacon, John W., Jr.; Goldsmith, John; and Gross, Lloyd W.: Effect of Slot Configuration and Disturbances From Slot or Environment on Laminar Flow Vehicles. Rep. No. NCL-68-46R (Contract N00017-67-C-1112), Northrop Corporate Labs., July 1968. (Available from DTIC as AD 851 246.)

40. Valsov, Ye V.; and Ginevskiy, A. S.: Effect of Acoustical Disturbances on the Transition of Laminar Boundary Layer to Turbulent. FTD-MT-24-0340-75, U.S. Air Force, Feb. 1975. (Available from DTIC as AD A007 446.)

41. Kachanov, Yu. S.; Kozlov, V. V.; Levchenko, V. Ya.; and Maksimov, V. P.: The Transformation of External Disturbances Into the Boundary Layer Waves. Sixth International Conference on Numerical Methods in Fluid Dynamics, Volume 90 of Lecture Notes in Physics, H. Cabannes, M. Holt, and V. Rusanov, eds., Springer-Verlag, 1979, pp. 299-307.

42. Braslow, Albert L.: A Review of Factors Affecting Boundary-Layer Transition. NASA TN D-3384, 1966.

43. Kachanov, Iu S.; Kozlov, V. V.; and Levchenko, V. A.: Generation and Development of Small Amplitude Disturbances in a Laminar Boundary Layer in the Presence of an Acoustic Field. Izv. Akad. Nauk Arm. SSR, Ser. Tekh. Nauk, Issue 3, no. 13, Oct. 1975, pp. 18-26.

44. Rogler, H.: The Interaction Between Vortex-Array Representations of Free-Stream Turbulence and Semi-Infinite Flat Plates. J. Fluid Mech., vol. 87, pt. 3, Aug. 15, 1978, pp. 583-606.

45. Benek, John Addison: The Effects of Periodic Free Stream Disturbances on the Flat Plate Boundary Layer. Ph. D. Diss., Univ. Tenn., 1975.

46. Werle, M. J.; Mook, D. T.; and Tang, H.: Effect of Free-Stream Vorticity on Boundary-Layer Stability. Phys. Fluids, vol. 16, no. 4, Apr. 1973, pp. 457-462.

47. Kapinos, V. M.; Levchenko, V. Ya.; Slitenko, A. F.; Kozlov, V. V.; and Volovel'skii, I. L.: Effect of Temperature Factor and Turbulence of the Impinging Stream on the Transition in the Boundary Layer With Gradient Flow. J. Eng. Phys., vol. 32, no. 3, Mar. 1977, pp. 393-398.

48. Gaponov, S. A.: Interaction Between a Supersonic Boundary Layer and Acoustic Disturbances. Fluid Dyn., vol. 12, no. 6, July 1978, pp. 858-862.

49. Hoffman, G. H.; and Lumley, J. L.: The Laminar Velocity Profile in a Flat Plate Boundary Layer With Surface Roughness. TM 77-150 (Contract No. N00017-73-C-1418), Appl. Res. Lab., Pennsylvania State Univ., May 1977. (Available from DTIC as AD A050 198.)

50. Dyban, Ye. P.; Epik, E. Ya.; and Suprun, T. T.: Characteristics of the Laminar Boundary Layer in the Presence of Elevated Free-Stream Turbulence. Fluid Mech. - Soviet Res., vol. 5, no. 4, July-Aug. 1976, pp. 30-36.

51. BCAC Preliminary Design Dep.: Evaluation of Laminar Flow Control System Concepts for Subsonic Commercial Transport Aircraft. NASA CR-158976, 1978.

52. Gruschka, H. D.: Periodisch Angeregte Grenzschichtstorungen Über Einer Ebenen Platte in Einer Wasserstromung. Acustica, vol. 16, no. 1, 1965/66, pp. 46-60.

53. Wallace, D. B.; and Spangler, J. G.: Disturbance Effects on Boundary Layer Transition in the Presence of a Strong Favorable Pressure Gradient. ATC Rep. No. B-94300/7CR-53 (Contract No. N000140-76-C-6627), Vought Corporation Advanced Technology Center, Inc., June 1977.

54. Savel'ev, Iu P.: Influence of External-Flow Turbulence on Laminar-Turbulent Transition for Some Classes of Self-Similar Flows. Inzh. Fiz. Zh., vol. 30, Mar. 1976, pp. 519-527.

55. Wilson, S. D. R.; and Gladwell, I.: The Stability of a Two-Dimensional Stagnation Flow to Three-Dimensional Disturbances. J. Fluid Mech., vol. 84, pt. 3, Feb. 13, 1978, pp. 517-527.

56. Wazzan, A. R.; Taghavi, H.; and Li, Y. Y.: Effect of Free Stream Vorticity on Spatial Stability of Incompressible Boundary Layers With Nonparallel Effects. Phys. Fluids, vol. 19, no. 3, Mar. 1976, pp. 362-365.

57. Rogler, Harold L.: The Coupling Between Freestream Disturbances, Driver Oscillations, Forced Oscillations, and Stability Waves in a Spatial Analysis of a Boundary Layer. Laminar-Turbulent Transition, AGARD-CP-224,Oct. 1977, pp. 16-1 - 16-14.

58. Gougat, Pierre; and Martin, Francoise: Influence D'une Deformation Periodique De Paroi Sur le Developpement des Instabilities Naturelles Conduisant a la Transition. Laminar-Turbulent Transition, AGARD-CP-224, Oct. 1977, pp. 18-1 - 18-9.

59. Pfenninger, Werner: Laminar Flow Control Laminarization. Special Course on Concepts for Drag Reduction, AGARD-R-654, June 1977, pp. 3-1 - 3-75.

60. Lekoudis, S. G.: Stability of Boundary Layers Over Permeable Surfaces. AIAA Paper 78-203, Jan. 1978.

61. Smith, A. M. O.: Feasibility Report - Laminar-Boundary-Layer Control. Rep. No. ES 26353 (Contract NOas 54-773C), Douglas Aircraft Co., Inc., July 31, 1956. (Available from DTIC as AD 148 307.)

62. Gibbings, J. C.; and Hall, D. J.: Criterion for Tolerable Roughness in a Laminar Boundary Layer. J. Aircr., vol. 6, no. 2, Mar.-Apr. 1969, pp. 171-173.

63. Von Doenhoff, Albert E.; and Braslow, Albert L.: The Effect of Distributed Surface Roughness on Laminar Flow. Boundary Layer and Flow Control, Volume 2, G. V. Lachmann, ed., Pergamon Press, Inc., pp. 657-681.

64. Braslow, Albert L.; and Knox, Eugence C.: Simplified Method for Determination of Critical Height of Distributed Roughness Particles for Boundary-Layer Transition at Mach Numbers From 0 to 5. NACA TN 4363, 1958.

65. Lachmann, G. V.: Aspects of Insect Contamination in Relation to Laminar Flow Aircraft. C.P. No. 484, British A.R.C., 1960.

66. Coleman, W. S.: Roughness Due to Insects. Boundary Layer and Flow Control, Volume 2, G. V. Lachmann, ed., Pergamon Press, 1961, pp. 682-747.

67. Carmichael, B. H.: Surface Waviness Criteria for Swept and Unswept Laminar Suction Wings. Rep. No. NOR-59-438 (BLC-123) (Contract AF33(616)-3168), Northrop Aircraft, Inc., Aug. 1959.

68. Jacobs, Eastman N.: Immediate Use of New Airfoil Sections of the Laminar-Flow Type. NACA WR L-521, 1940. (Formerly NACA MR.)

69. Fowell, L. R.; and Antonatos, P. P.: A. Some Results From the X-21A Program. Part 2: Laminar Flow Control Flight Test Results on the X-21A, Recent Developments in Boundary Layer Research - Part IV, AGARDograph 97, May 1965.

70. Zozulya, V. B.; and Cheranovskiy, O. R.: Control of Laminar Flow Past a Wing in Free Flight. Fluid Mech. - Soviet Res., vol. 2, no. 5, Sept.-Oct. 1973, pp. 16-20.

71. Braslow, Albert L.; and Muraca, Ralph J.: A Perspective of Laminar-Flow Control. AIAA Paper 78-1528, Aug. 1978.

72. Owen, P. R.; and Randall, D. G.: Boundary Layer Transition on a Sweptback Wing: Effect of Incidence. Tech. Memo. No. Aero. 375, British R.A.E., Oct. 1953.

73. Burrows, F. M.: Characteristics of the Flow Field Over the Mid-Upper Fuselage of Lancaster P.A. 474. Note No. 36, Coll. of Aeronaut., Cranfield (England), Jan. 1956.

74. Burrows, F. M.: Equipment Used for Boundary Layer Measurements in Flight. Note No. 49, Coll. of Aeronaut., Cranfield (England), July 1956.

75. Allen, L. D.; and Burrows, F. M.: Flight Experiments on the Boundary Layer Characteristics of a Swept Back Wing. Rep. No. 104, Coll. of Aeronaut., Cranfield (England), July 1956.

76. Burrows, F. M.: A Theoretical and Experimental Study of the Boundary Layer Flow on a 45° Swept Back Wing. Rep. No. 109, Coll. of Aeronaut., Cranfield (England), Oct. 1956.

77. Walton, J.: Addendum to a Theoretical and Experimental Study of the Boundary Layer Flow on a 45° Swept Back Wing. Rep. No. 109 Addendum, Coll. of Aeronaut., Cranfield (England), Nov. 1957.

78. Landeryou, R. R.; and Porter, P. G.: Further Tests of a Laminar Flow Swept Wing With Boundary Layer Control by Suction. Rep. Aero. No. 192, Coll. of Aeronaut., Cranfield (England), May 1966.

79. Landeryou, R. R.; and Trayford, R. S.: Flight Tests of a Laminar Flow Swept Wing With Boundary Layer Control by Suction. CoA. Rep. Aero. No. 174, Coll. of Aeronaut., Cranfield (England), June 1964.

80. Russell, W. R.: Analysis of Low-Speed Wind Tunnel Tests of a 30° Swept, Laminar, Suction Wing. NOR-61-233 (Contract AF33(600)-42052), Northrop Corp., Sept. 1961.

81. Pfenninger, W.; Gross, L. W.; Bacon, J. W., Jr.; and Tucker, V. L.: Experimental Investigation of a 30° Swept 12%-Thick Laminar Suction Wing in the NASA Ames 12-Foot Pressure Wind Tunnel. Rep. No. NOR-60-108 (BLC-129), Northrop Corp., Oct. 1961.

82. Gault, Donald E.: An Experimental Investigation of Boundary-Layer Control for Drag Reduction of a Swept-Wing Section at Low Speed and High Reynolds Numbers. NASA TN D-320, 1960.

83. Gross, L. W.; Bacon, J. W., Jr.; and Tucker, V. L.: Experimental Investigation and Theoretical Analysis of Laminar Boundary Layer Suction on a 30° Swept, 12-Percent-Thick Wing in the NASA Ames 12-Foot Pressure Wind Tunnel. Summary of Laminar Boundary Layer Control Research, Volume I, ASD-TDR-63-554, U.S. Air Force, Mar. 1964, pp. 96-110. (Available from DTIC as AD 605 185.)

84. Boltz, Frederick W.; Kenyon, George C.; and Allen, Clyde Q.: The Boundary-Layer Transition Characteristics of Two Bodies of Revolution, a Flat Plate, and an Unswept Wing in a Low-Turbulence Wind Tunnel. NASA TN D-309, 1960.

85. Boltz, Frederick W.; Kenyon, George C.; and Allen, Clyde Q.: Effects of Sweep Angle on the Boundary-Layer Stability Characteristics of an Untapered Wing at Low Speeds. NASA TN D-338, 1960.

86. Pfenninger, W.; Gross, Lloyd; and Bacon, John W., Jr.: Experiments on a 30° Swept 12%-Thick Symmetrical Laminar Suction Wing in the 5-Ft. by 7-Ft. Michigan Tunnel. Rep. No. BLC-93, Rep. No. NAI-57-317, Northrop Aircraft, Inc., Feb. 1957.

87. Bacon, J. W., Jr.; Tucker, V. L.; and Pfenninger, W.: Experiments on a 30° Swept, 12% Thick Symmetrical Laminar Suction Wing in the 5- by 7-Foot University of Michigan Tunnel. Rep. No. NOR-59-328 (BLC-119), Northrop Aircraft, Inc., Aug. 1959.

88. Hyde, D.: Pressure and Boundary Layer Measurements on a Tapered Swept Wing in Flight. CP No. 560, British A.R.C., 1961.

89. Pindar, A. C. S.; and Collingbourne, J. R.: Pressure Plotting and Balance Measurements in the High Speed Wind Tunnel on a Half-Model of a 90-Deg-Apex Delta Wing With Fuselage. R. & M. No. 2844, British A.R.C., 1954.

90. Pfenninger, W.: Summary Report About the Investigation of a 10-Ft. Chord 33° Swept Low Drag Suction Wing at High Reynolds Numbers. Northrop paper presented to Air Force Advisory Group, Oct. 14, 1965.

91. Carlson, J. C.; and Bacon, J. W., Jr.: Influence of Acoustical Disturbances in the Suction Ducting System on the Laminar Flow Control Characteristics of a 33° Swept Suction Wing. NOR-65-232, Northrop Corp., Aug. 1965.

92. Carlson, J. C.: Low Drag Boundary Layer Suction Experiments Using a 33° Swept 15% Thick Laminar Suction Wing With Suction Slots Normal to the Leading Edge. NOR-64-281, Northrop Corp., Nov. 1964. (Available from DTIC as AD 482 068.)

93. Franco, B. G.: Data Report of a High Reynolds Number Wind Tunnel Test of an Acoustically Instrumented Laminar Flow Control 33° Swept Suction Wing Conducted at the Ames Research Center 12' Pressure Tunnel - August 1965. NOR-65-312, Northrop Corp., 1965 .

94. Carlson, J. C.: Investigation of the Laminar Flow Control Characteristics of a 33° Swept Suction Wing at High Reynolds Numbers in the NASA Ames 12-Foot Pressure Wind Tunnel in August 1965. NOR-66-58, Northrop Corp., Jan. 1966.

95. Whites, R. C.; Sudderth, R. W.; and Wheldon, W. G.: Laminar Flow Control on the X-21. Astronaut. & Aeronaut., vol. 4, no. 7, July 1966, pp. 38-43.

96. LFC Aircraft Design Data Laminar Flow Control Demonstration Program. Final Report, NOR-67-136 (AF 33/657-13930), Northrop Corp., June 1967. (Available from DTIC as AD 819 317.)

97. Stark, W. W.: LFC Summary Flight Test Report - Laminar Flow Control Airplane Demonstration Program. Advanced Technology Program System 659A. NOR-61-134 (Contract AF 33(600)-42052), Northrop Corp., Apr. 1964. (Available from DTIC as AD 440 344.)

98. Tye, W.: The Effect of Smooth Wings on Weight and Performance. Rep. No. S.M.E.3234, British R.A.E., Oct. 1942.

99. Lekoudis, Spyridon G.: Stability of Three-Dimensional Compressible Boundary Layers Over Wings With Suction. AIAA Paper 79-0265, Jan. 1979.

100. Mack, Leslie M.: On the Stability of the Boundary Layer on a Transonic Swept Wing. AIAA Paper 79-0264, Jan. 1979.

101. Nayfeh, Ali H.: Stability of Three-Dimensional Boundary Layers. AIAA Paper 79-0262, Jan. 1979.

TABLE I.- SUMMARY OF LOW-DISTURBANCE SWEPT-WING TRANSITION DATA

Authors and references	Configuration	Measurements	Comments and results
Burrows, Allen, Walton, Landeryou, Porter, Trayford (refs. 73 to 79)	Dorsal fin mounted on upper fuselage of Avro Anson, Lancaster, or Lincoln aircraft; wing sweep of $42^{\circ}35'$ and 45°; initially no suction; later, slot suction	Surface pitot; boundary-layer profiles; surface pressures	Well documented, an excellent set of experiments with sweep; essentially 3 separate studies: (1) 1.2-m chord, unsucked, Avro Anson (ref. 75); (2) 2.2-m chord, unsucked, Avro Lancaster (ref. 76); (3) 2.5-m chord, tapering to 1.7 m, slot suction, Avro Lincoln (ref. 78); transition given as a function of R_c, α, span
Pfenninger, Gault, Gross, Bacon, Russell, Tucker (refs. 80 to 83)	30° swept wing (NACA 66-012) with 93 spanwise suction slots; tested in Ames 12 Foot Pressure Wind Tunnel; 1.9-m chord	Surface pressure; suction distribution; wake surveys; microphones	Contoured end plates used; airfoil coordinates given; achieved full-chord laminar flow with suction to $R_c = 29 \times 10^6$
Boltz, Kenyon, Allen (refs. 84 and 85)	Variable sweep (Λ from 10° to 50°) NACA 64_2A015 wing without suction in Ames 12 Foot Pressure Wind Tunnel; 1.2-m chord	Surface pressure; microphones (for transition detection); surface hot wires	Surface waviness measured; transition location was a function of fan blade angle, sound level in tunnel; study was well documented; transition Reynolds numbers to 15×10^6
Pfenninger, Bacon, Gross, Tucker (refs. 86 and 87)	30° swept, NACA 66-012 wing with slot suction in 5- by 7-Foot University of Michigan Tunnel; 2.1-m chord	Surface pressure; suction distribution; wake surveys	This wing later tested in Ames tunnel (refs. 81 and 82); transition Reynolds numbers to 12×10^6
Hyde (ref. 88)	Dorsal fin mounted on upper fuselage of Avro Lancaster aircraft; 40° swept (quarter-chord station), tapered, RAE 102 symmetric airfoil without suction; coordinates given in reference 89	Surface pressure; boundary-layer profiles	Chord tapers from 2.4 m down to 1.3 m; surface pressures tabulated and plotted; experiments actually in another in Cranfield series and came between references 77 and 78; transition onset essentially in agreement with Owen and Randall criterion
Carlson, Pfenninger, Franco, Bacon (refs. 90 to 94)	33° swept wing, 15-percent thick, with spanwise suction slots tested in Ames 12 Foot Pressure Tunnel	Surface pressure; microphone data	Slots/surface finish may not be optimized; surface pressure had spatial oscillation around $x/c \approx 0.08$; wing was also tested in Norair 7- by 10-Foot Wind Tunnel (ref. 91); transition given as a function of R_c; transition Reynolds numbers to 40×10^6
Stark, et al. (refs. 95 to 98)	30° swept wing with spanwise suction slots tested on Northrop X-21A aircraft	Wake surveys; microphone data; hot film	Detailed knowledge of local suction rates evidently lacking; some estimates available (e.g., page 42 of ref. 95); transition Reynolds numbers to 47×10^6

TABLE II.- COMPARISON OF INTEGRATED AMPLIFICATION RATIOS

FOR SWEPT-WING WIND-TUNNEL AND FLIGHT DATA

Data source	Λ, deg	R_C	$(x/c)_T$	Envelope method		Fixed wavelength/ frequency method			Case identification
				f, cps	n	λ/c	f, cps	n	
Ames swept-wing tunnel experiments, no suction (refs. 80 to 85) - analysis from reference 15	30	16.1×10^6	0.190	0	9.6	-------	----	----	30C
	30	12.3	.490	0	10.3	0.00125	0	6.8	30B
	40	10.6	.370	0	11.5	.00175	0	7.2	40D
	40	8.4	.500	0	9.7	.00225	0	6.8	40A
	20	22.4	.370	0	9.2	-------	----	----	20E
Cranfield flight experiments, no suction (ref. 76)	45	9.5	0.120	750	10.6	0.00150	250	6.8	$\alpha = 0^\circ$
	45	11.7	.070	1000	10.8	.00100	750	6.8	$\alpha = 0^\circ$
	45	9.5	.090	500	10.3	.00125	500	7.5	$\alpha = 2^\circ$
	45	11.7	.045	1400	11.0	.00100	1200	9.2	$\alpha = 2^\circ$
	45	9.5	.040	1000	8.6	.00075	750	7.7	$\alpha = 4^\circ$
	45	9.5	.090	750	8.7	.00200	600	6.1	$\alpha = -2^\circ$
	45	11.7	.055	1250	7.6	.00100	1000	6.2	$\alpha = -2^\circ$
	45	9.5	.090	750	9.7	.00200	600	7.5	$\alpha = -4^\circ$
X-21 data, suction (refs. 95 to 97)	30	22.5	Laminar	250	>1.5	0.00150	250	>1.5	$C_L = 0.3$; $M_\infty = 0.8$
Ames 33° swept wing, suction (refs. 90 to 94)	33	29.6	Laminar	0	>3.5	0.00150	0	>2.9	$\alpha = 1.5^\circ$
Michigan 30° swept wing, suction (refs. 86 to 87)	30	10.6	Laminar	250	>11.3	0.00300	250	>6.4	$\alpha = 0^\circ$

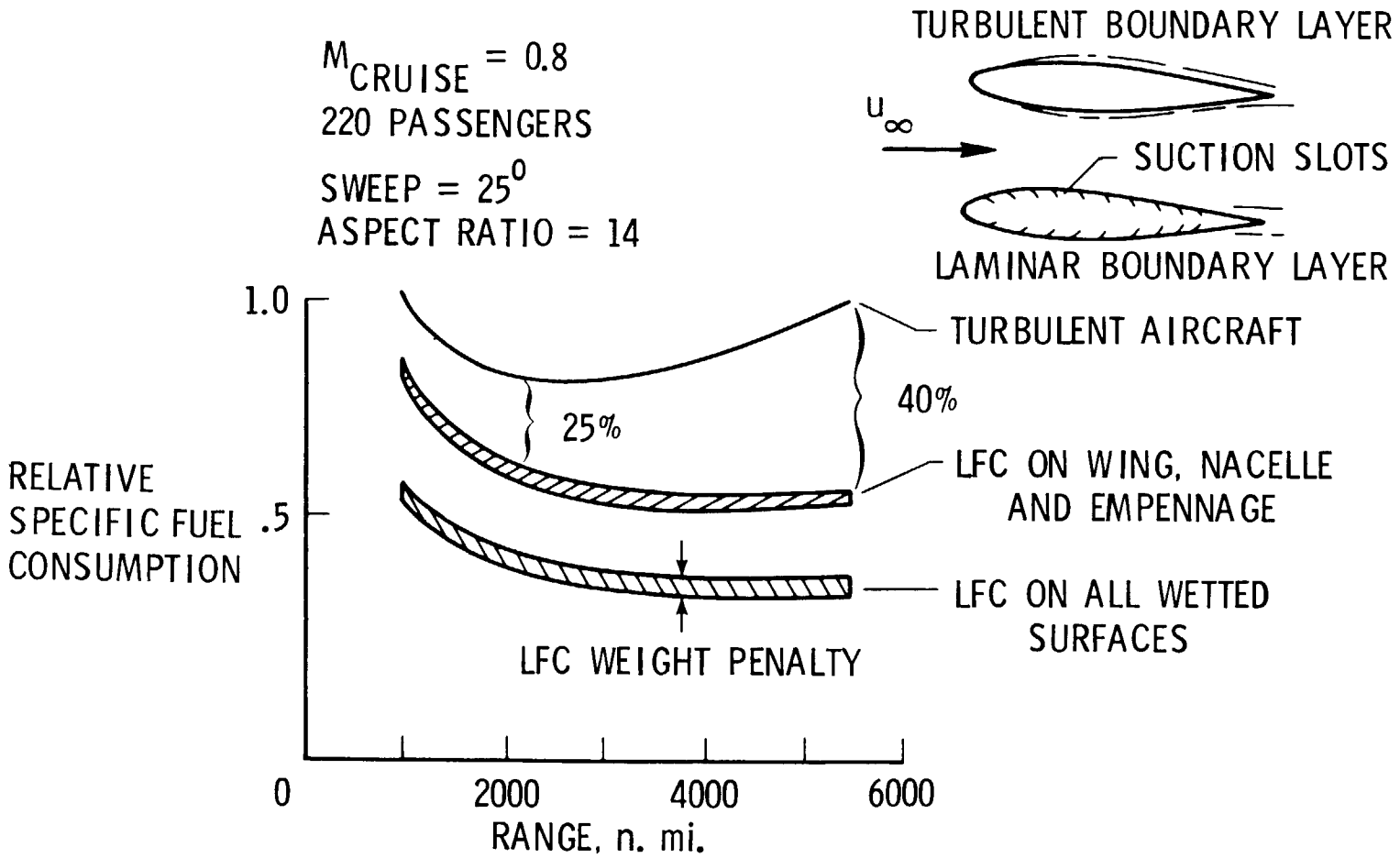

Figure 1.- Laminar-flow-control fuel conservation potential using suction.

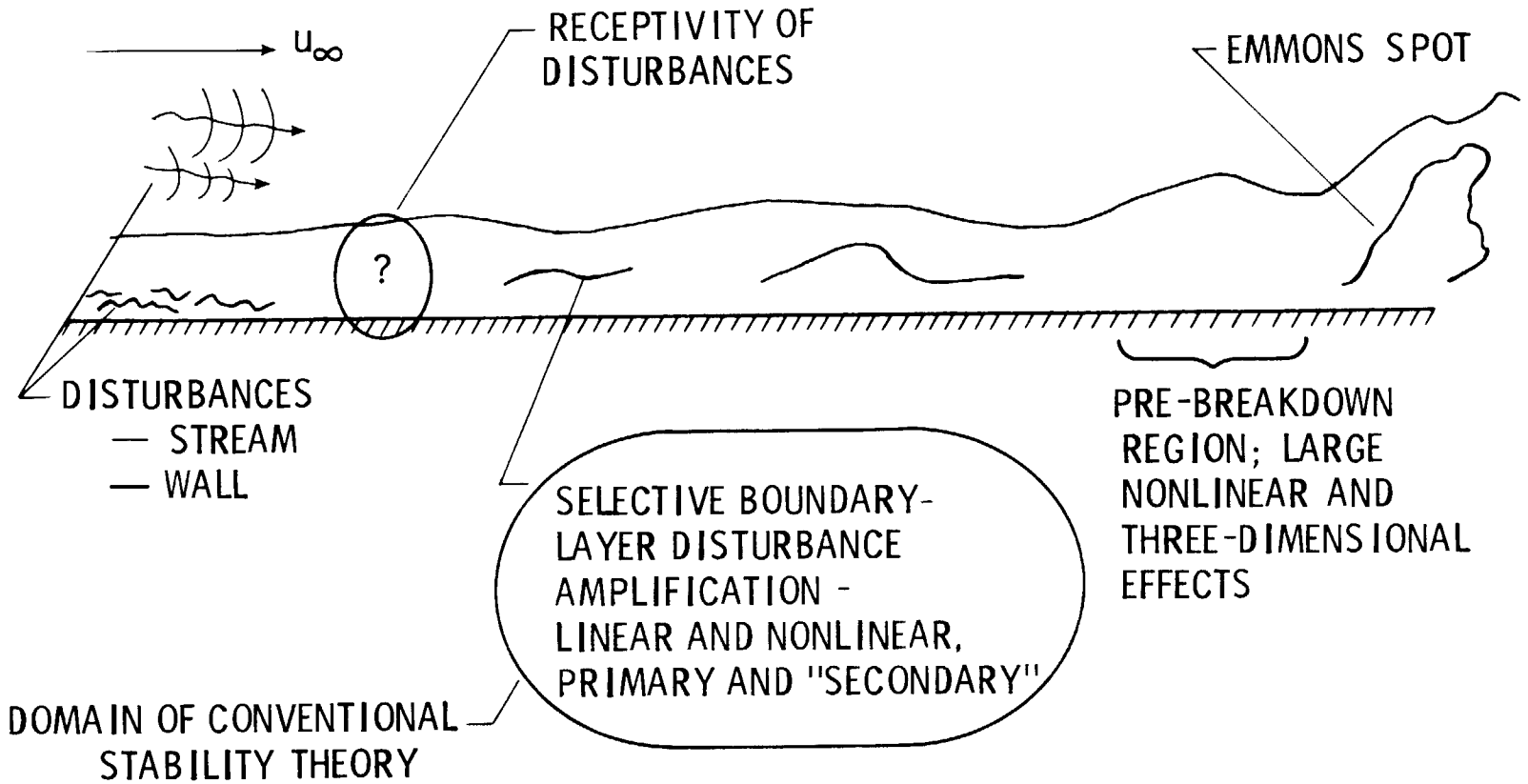

Figure 2.- Anatomy of transition process.

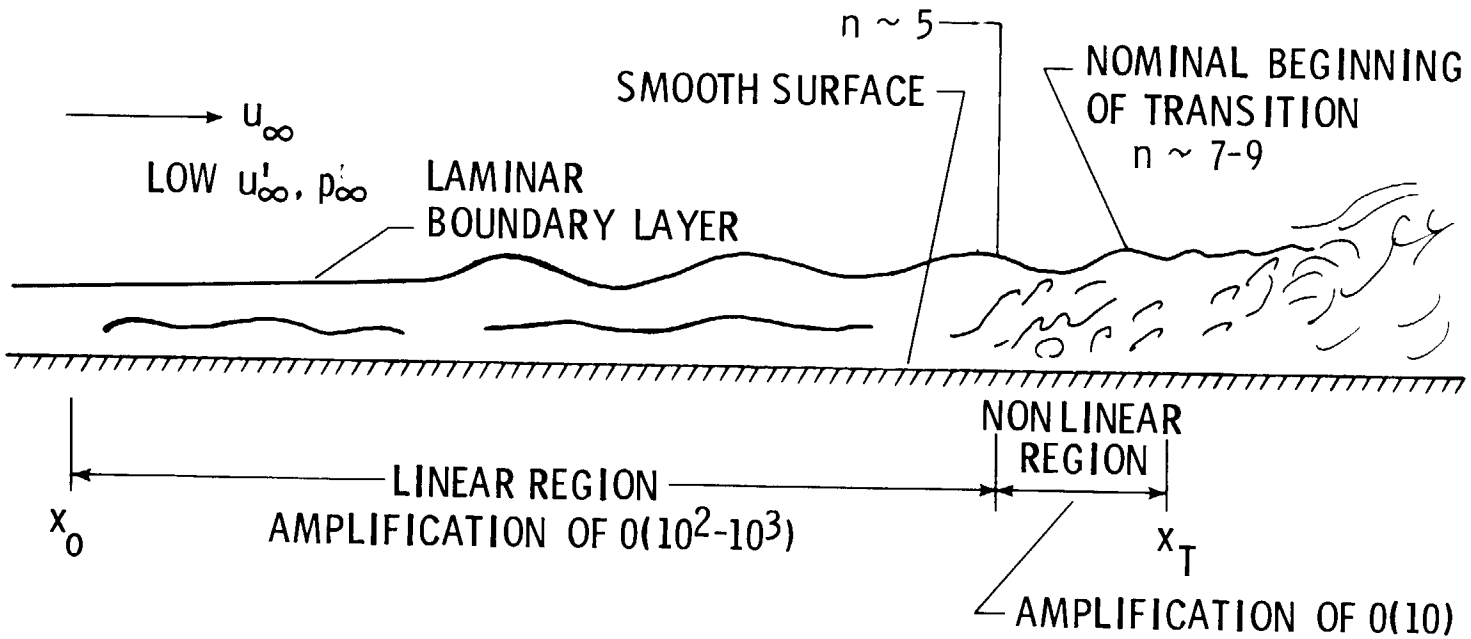

Figure 3.- Growth of disturbances within a laminar boundary layer; low background disturbance level.

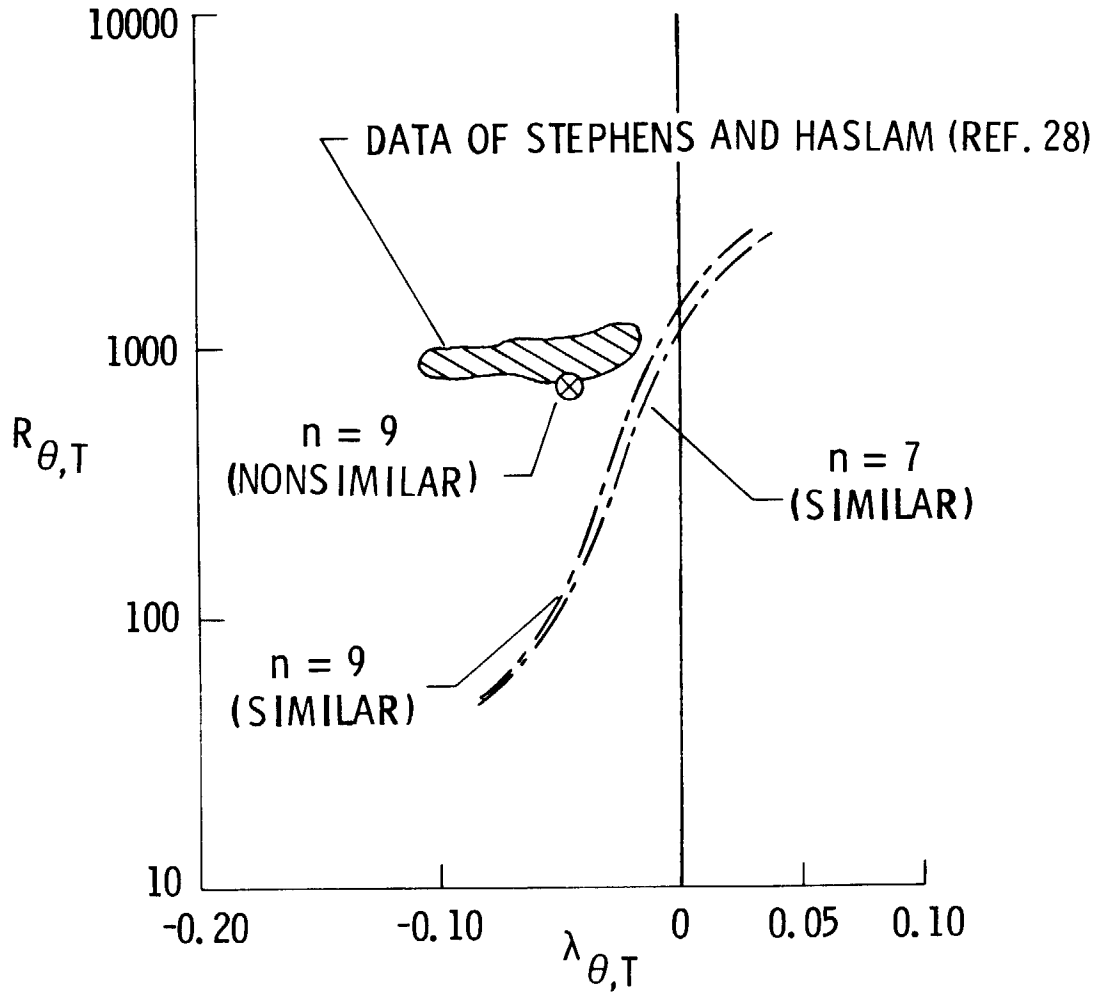

Figure 4.- Effect of pressure gradient on beginning of transition on two-dimensional airfoils.

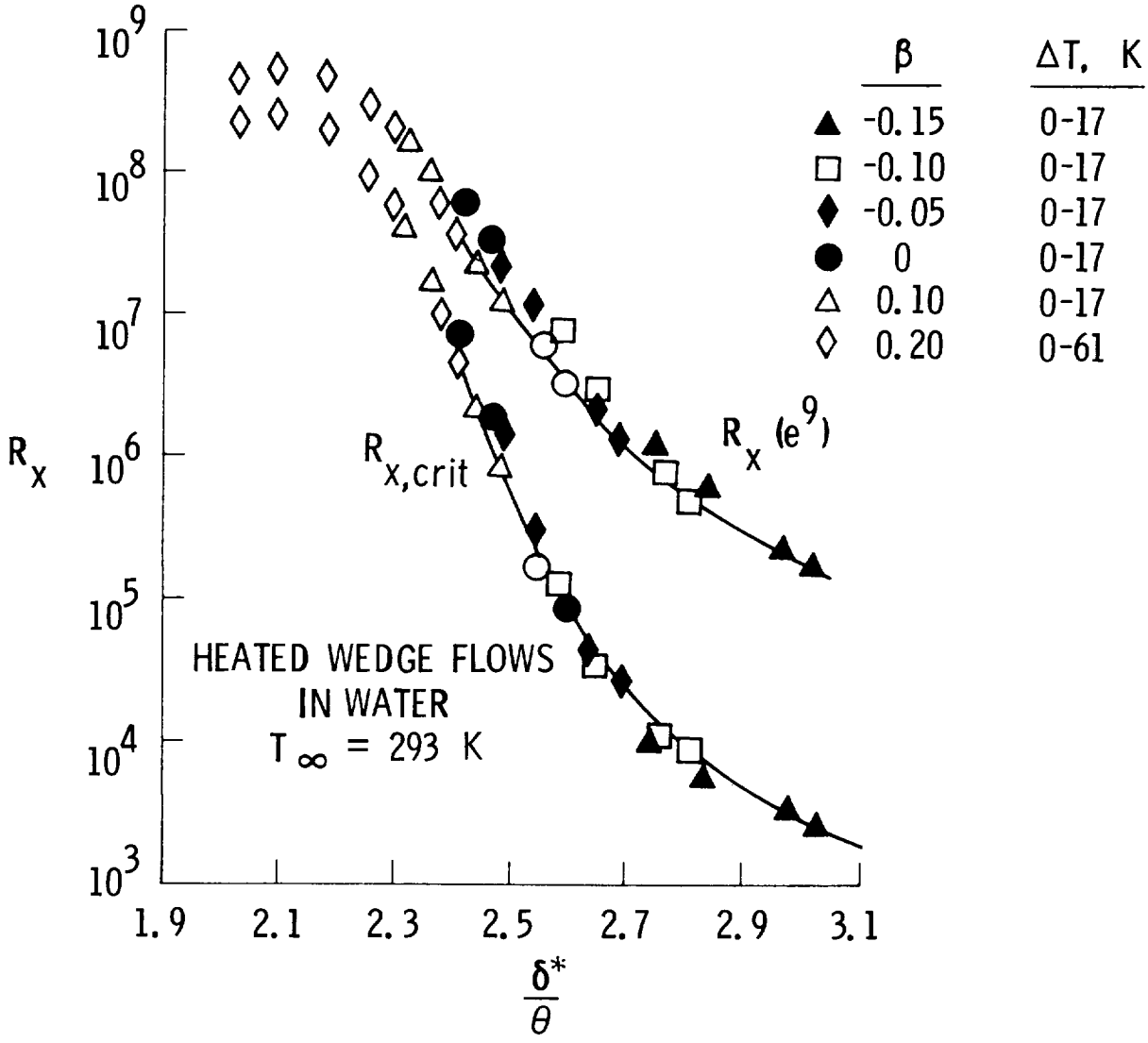

Figure 5.- Critical and transitional Reynolds numbers (based on e^9) as function of shape factor (ref. 29).

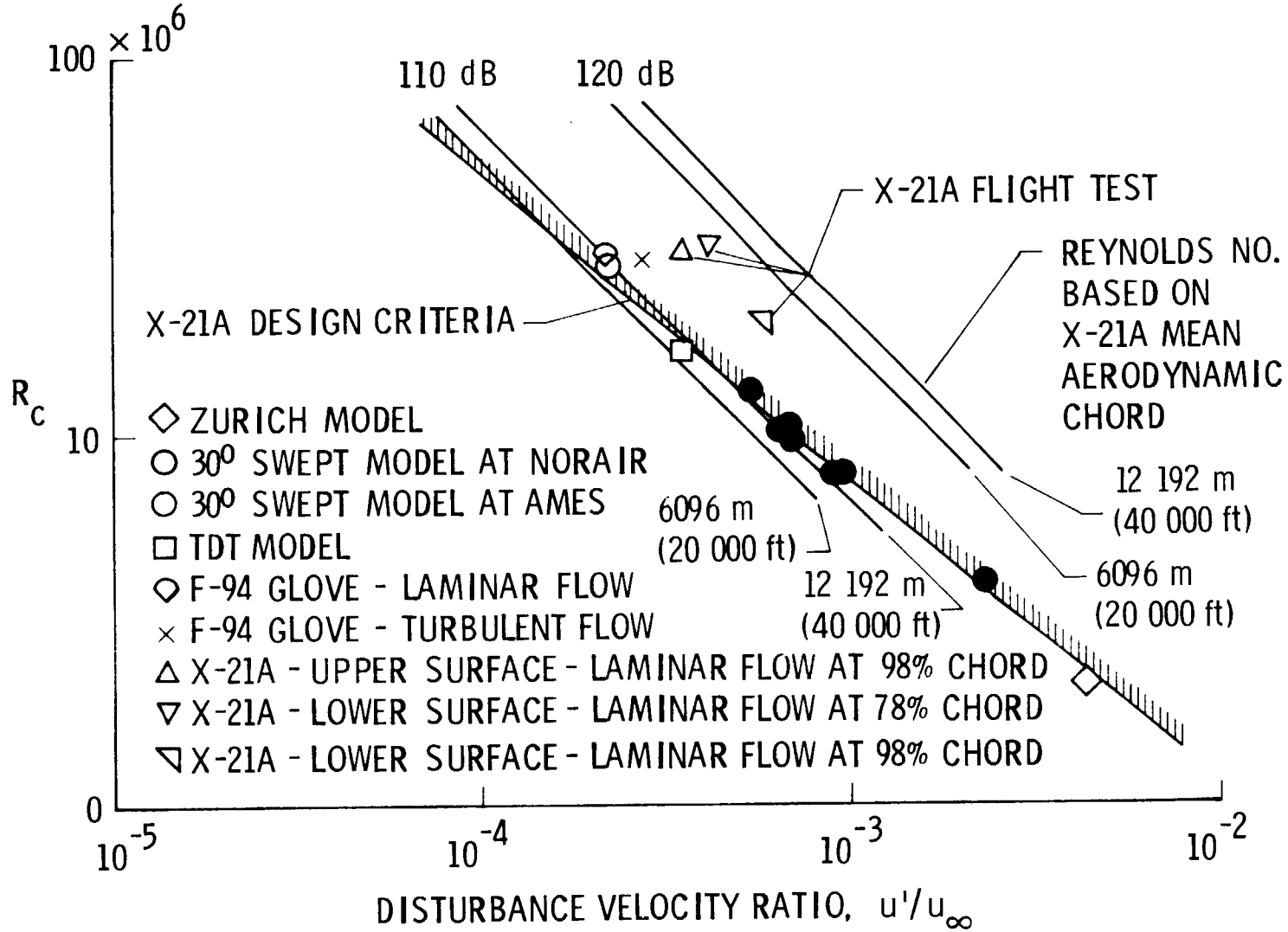

Figure 6.- Critical disturbance levels (ref. 69).

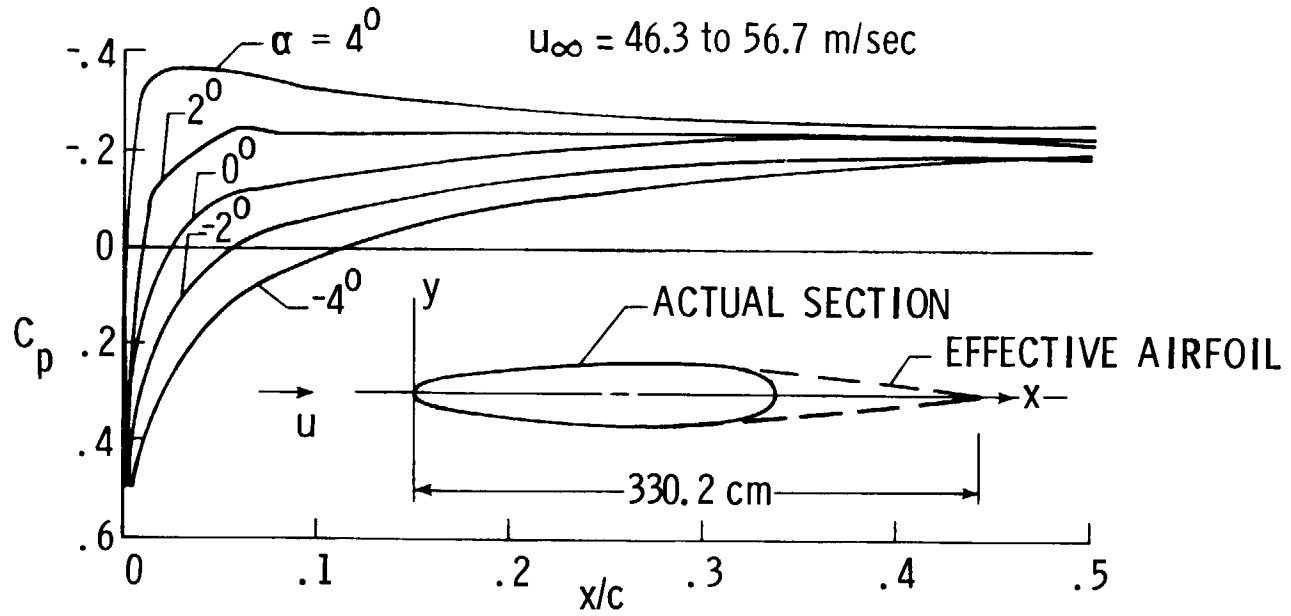

Figure 7.- Surface pressure distributions on Cranfield 45° swept wing tested on Avro Lancaster airplane. U_∞ = 46.3 to 56.7 m/sec.

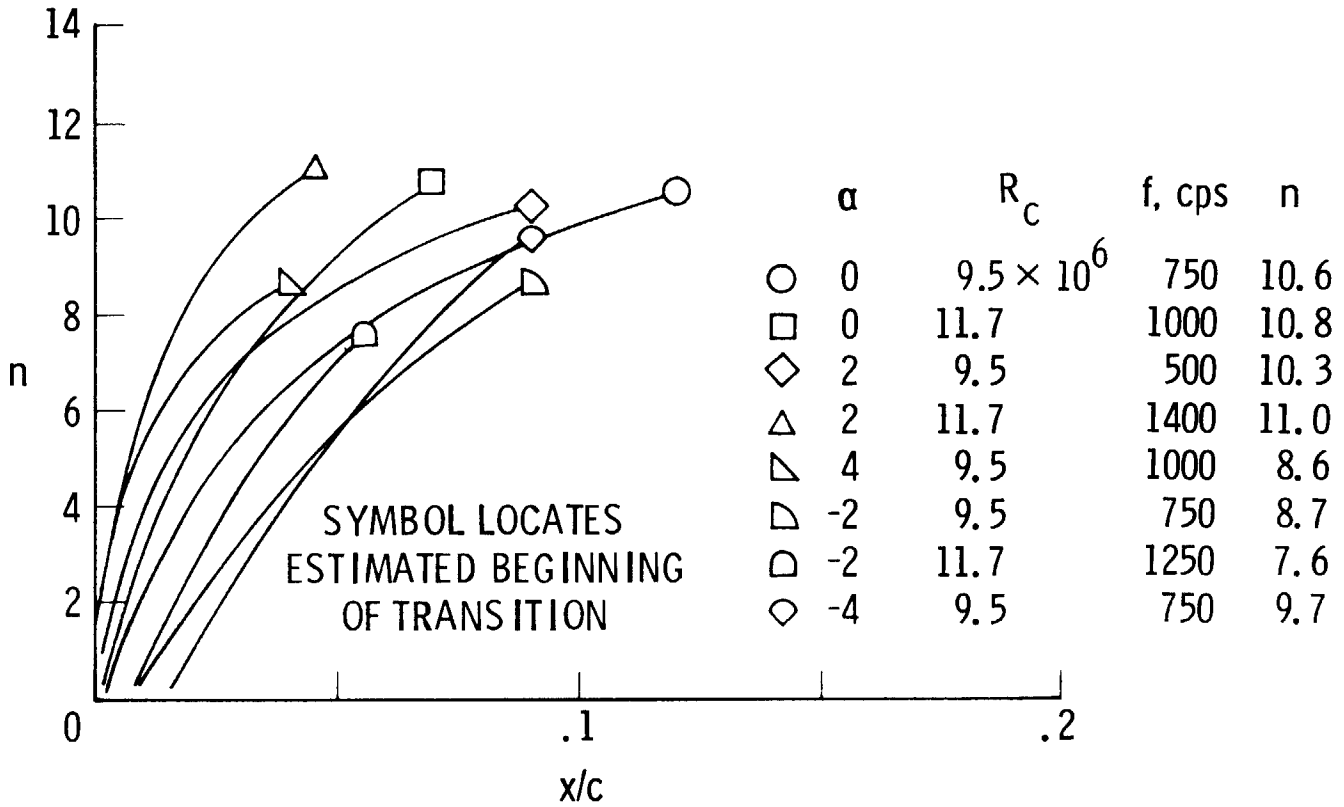

Figure 8.- Integrated amplification ratios on Cranfield 45° swept wing by envelope method.

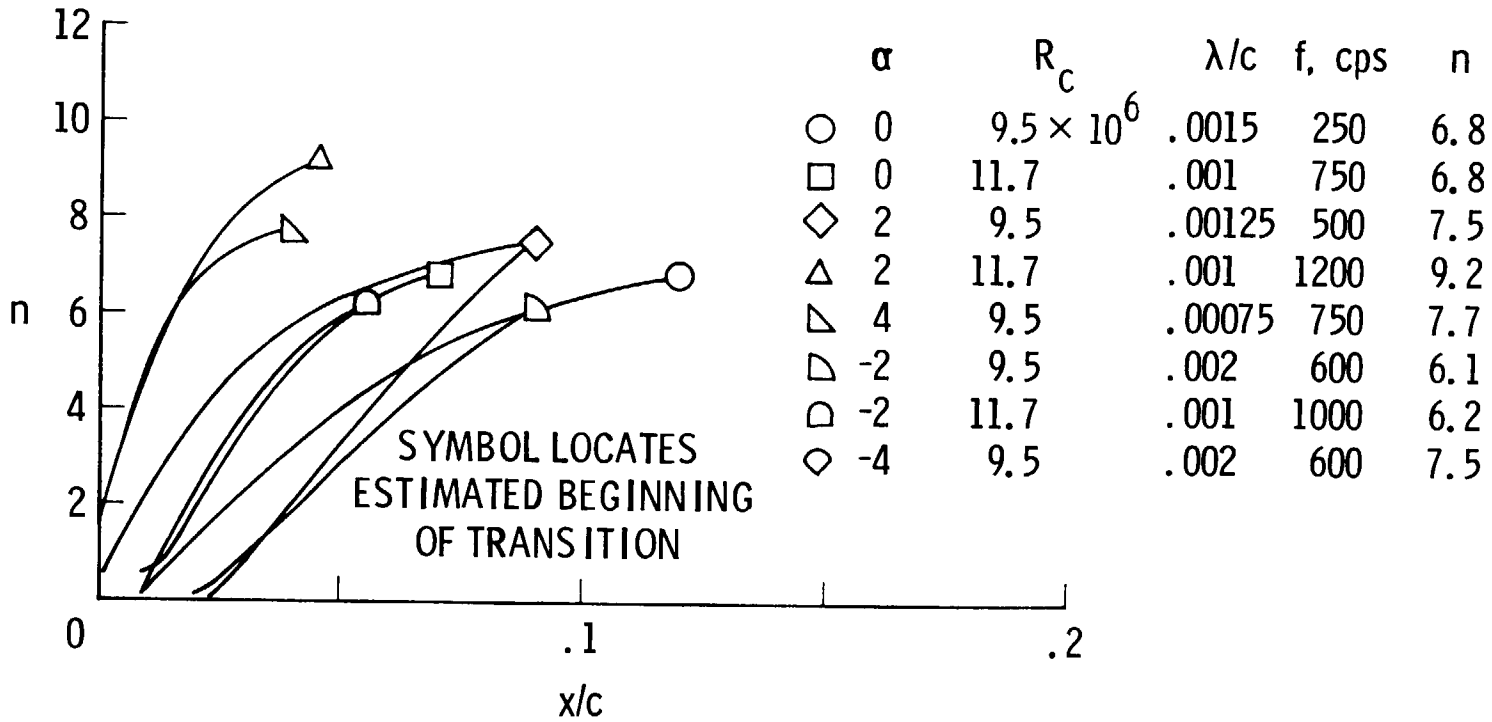

Figure 9.- Integrated amplification ratios on Cranfield 45° swept wing by fixed wavelength/frequency method.

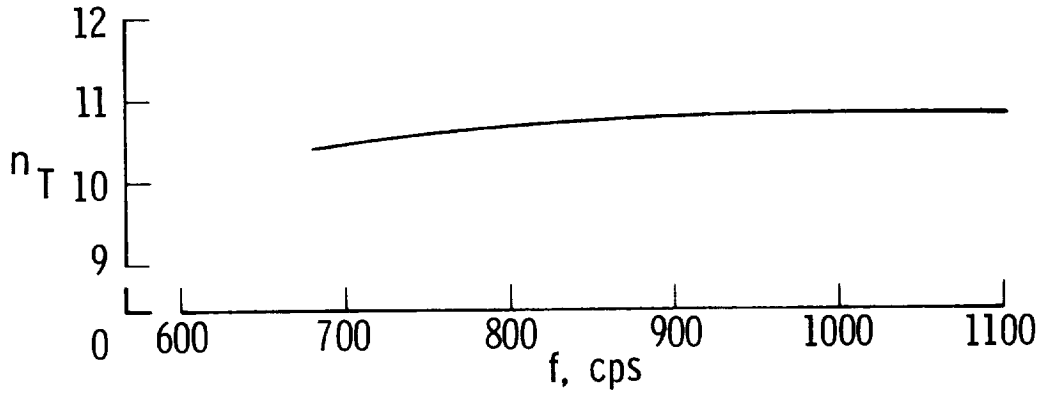

(a) Envelope method.

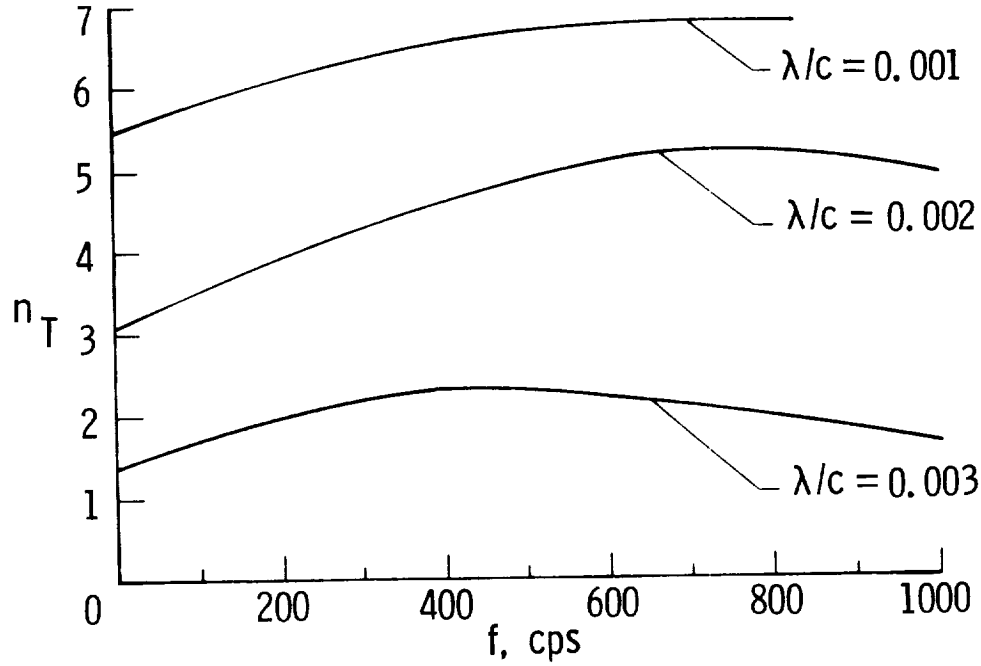

(b) Fixed wavelength/frequency method.

Figure 10.- Influence of frequency on integrated amplification ratios at transition for Cranfield 45° swept wing. $\alpha = 0^{\circ}$; $R_c = 11.7 \times 10^6$.

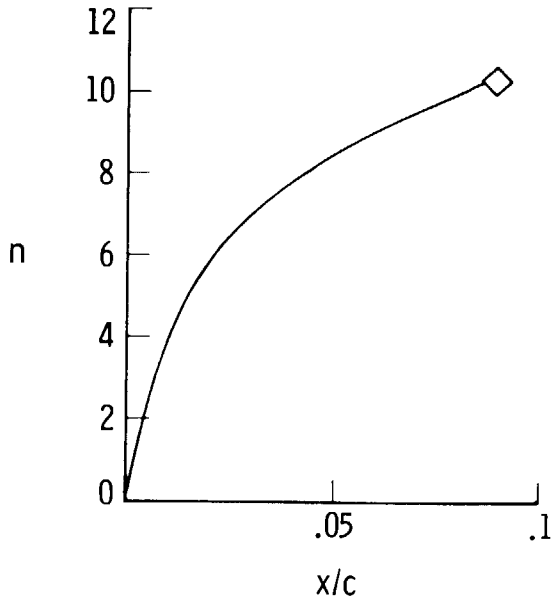

(a) Integrated amplification ratio.

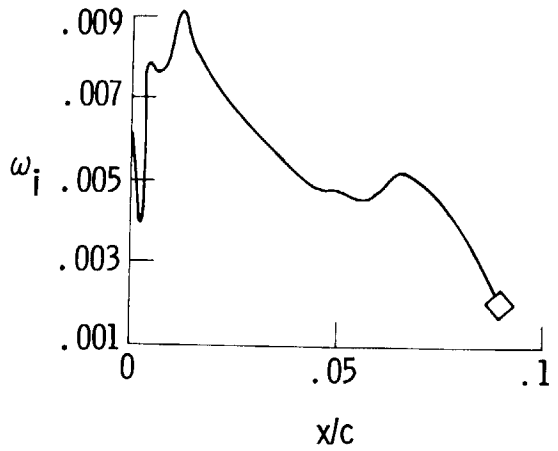

(b) Local disturbance amplification ratio.

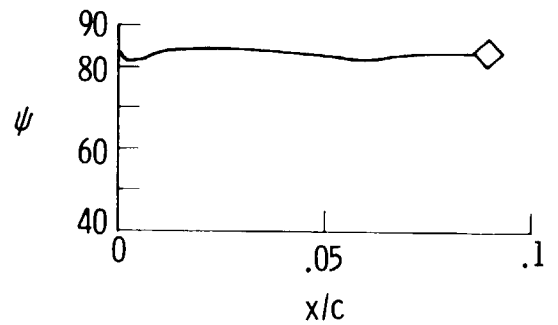

(c) Wave angle.

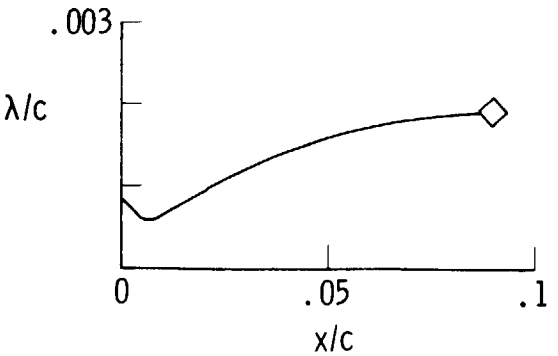

(d) Wavelength.

Figure 11.- Stability characteristics for Cranfield 45° swept wing by envelope method. $\alpha = 2^{\circ}$; $R_c = 9.5 \times 10^6$; f = 500 cps.

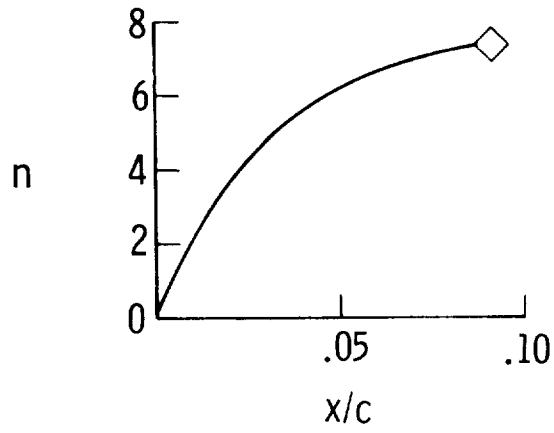

(a) Integrated amplification ratio.

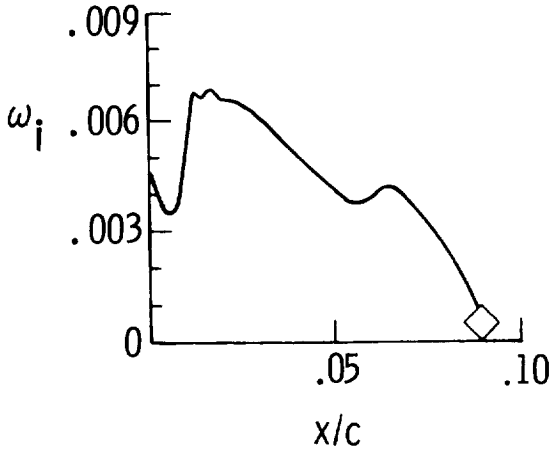

(b) Local disturbance amplification ratio.

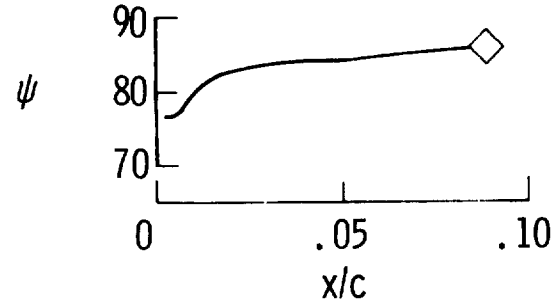

(c) Wave angle.

Figure 12.- Stability characteristics for Cranfield 45° swept wing by fixed wavelength/frequency method. $\alpha \cong 2^{\circ}$; $R_c = 9.5 \times 10^6$; $\lambda/c = 0.00125$; f = 500 cps.

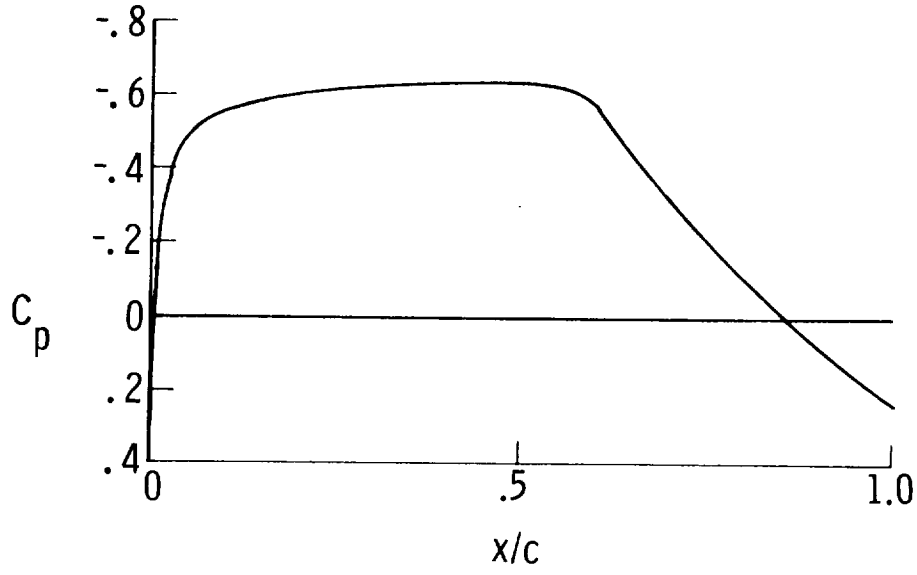

(a) Pressure distribution.

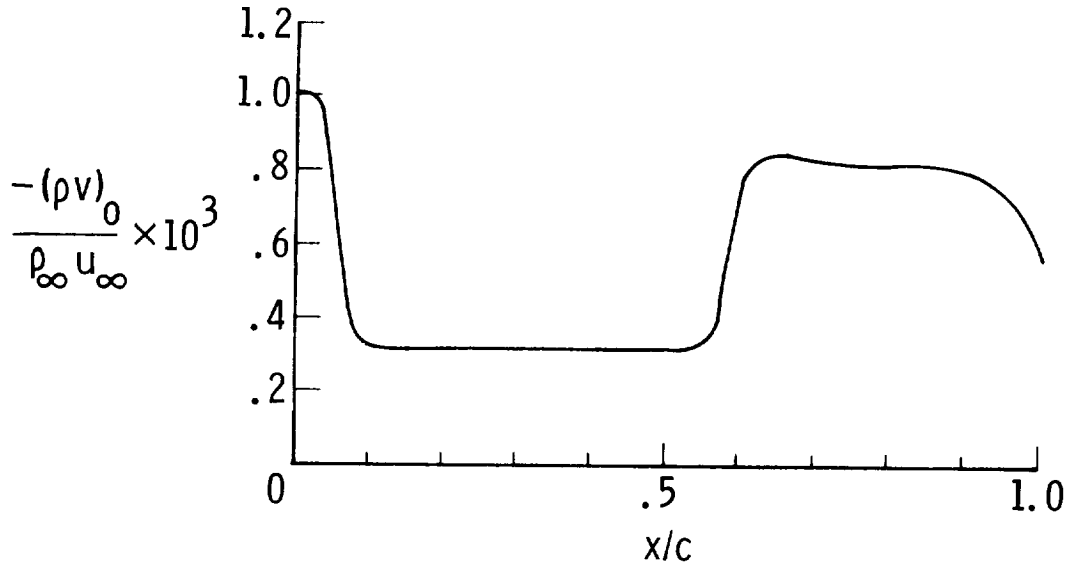

(b) Suction distribution.

Figure 13.- Pressure and suction distributions on Northrop X-21 wing. $M_\infty = 0.8$; $R_C = 22.5 \times 10^6$; and $C_L = 0.3$.

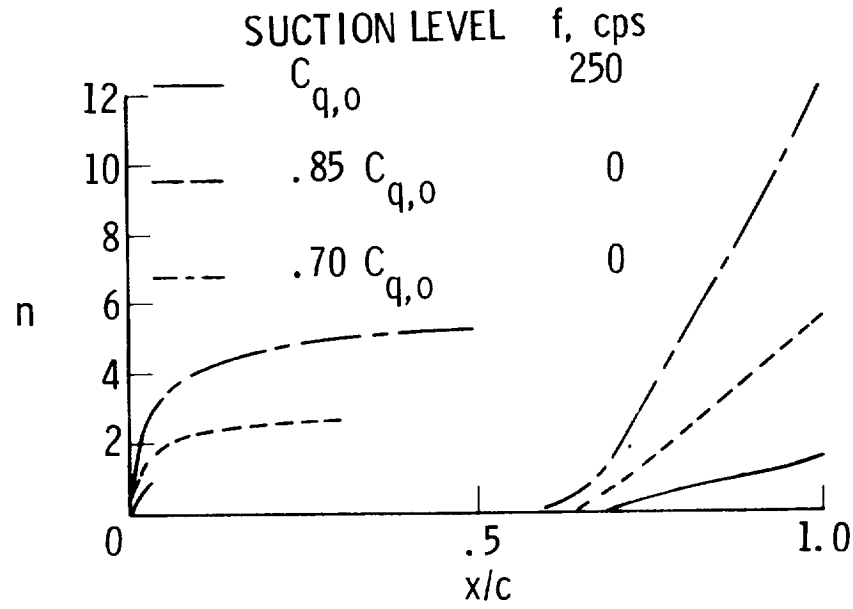

(a) Integrated disturbance amplification ratio along airfoil surface.

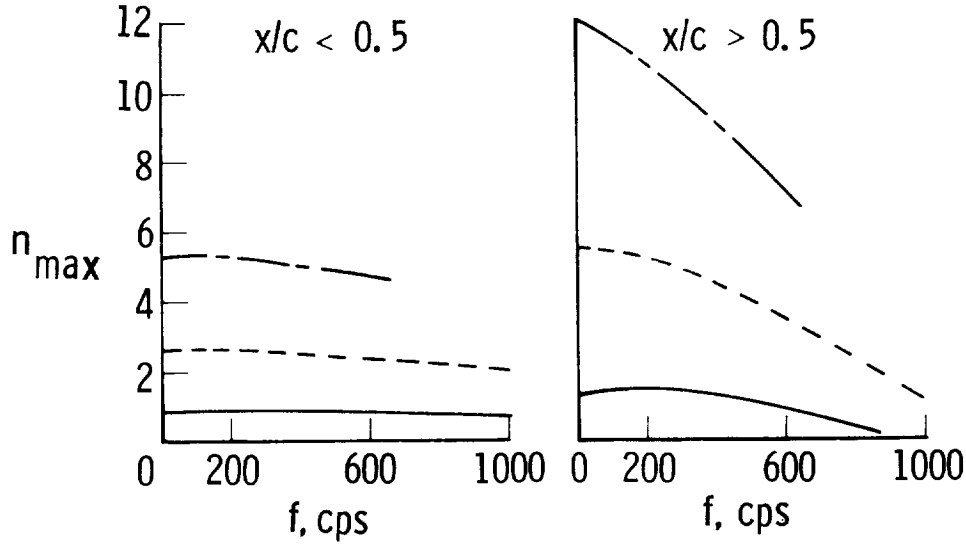

(b) Effect of frequency on maximum amplification ratios.

Figure 14.- Sensitivity of integrated disturbance amplification ratios on Northrop X-21 wing to suction level by envelope method.

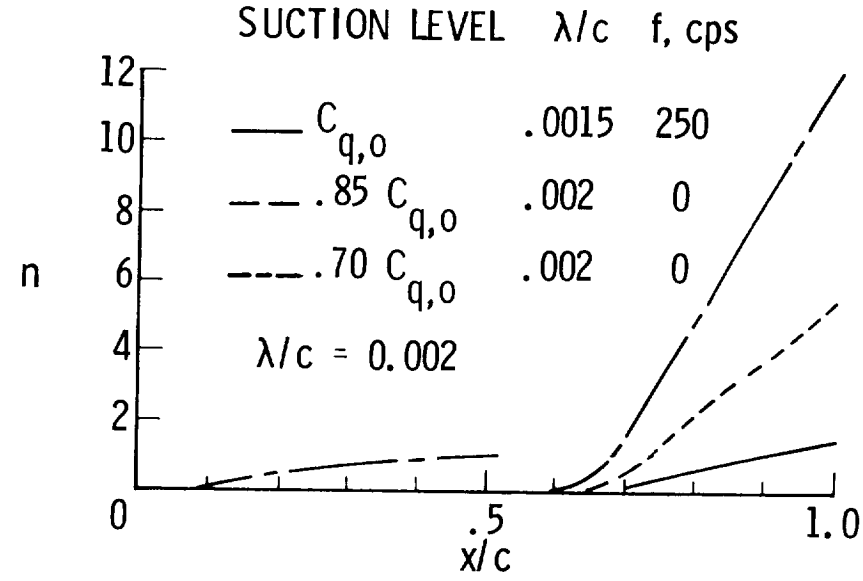

(a) Integrated disturbance amplification ratios along airfoil surface.

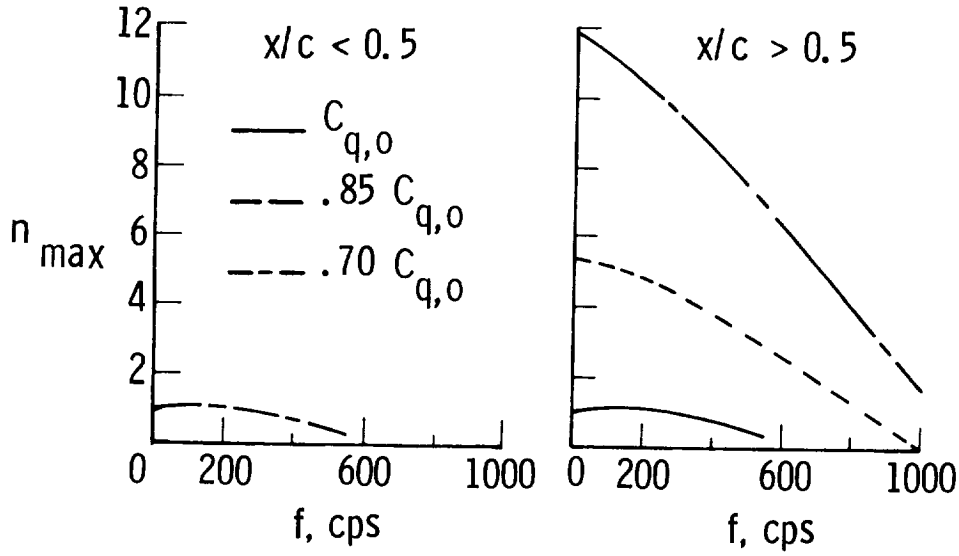

(b) Effect of frequency on maximum amplification ratios.

Figure 15.- Sensitivity of integrated disturbance amplification ratios on Northrop X-21 wing to suction level by fixed wavelength/frequency method.

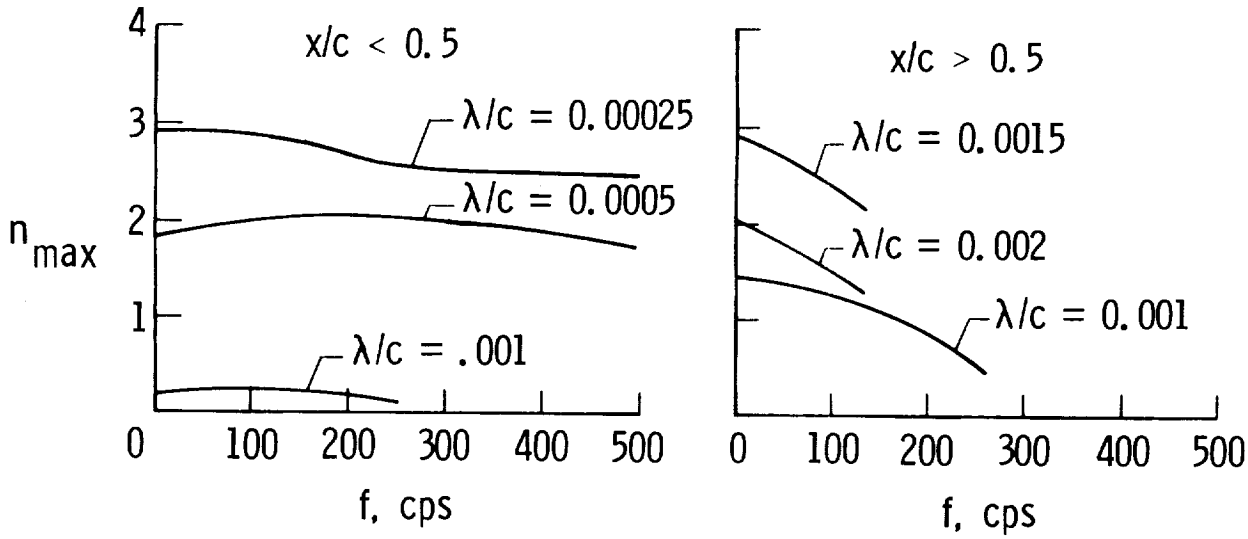

Figure 19.- Maximum integrated amplification ratios on Ames 33° swept wing by fixed wavelength/frequency method.

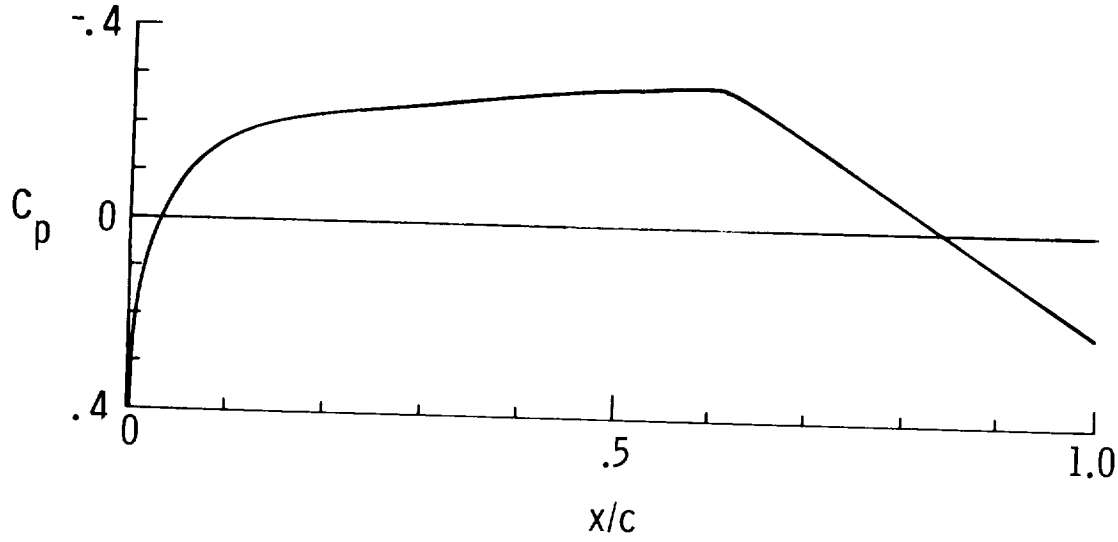

(a) Pressure distribution.

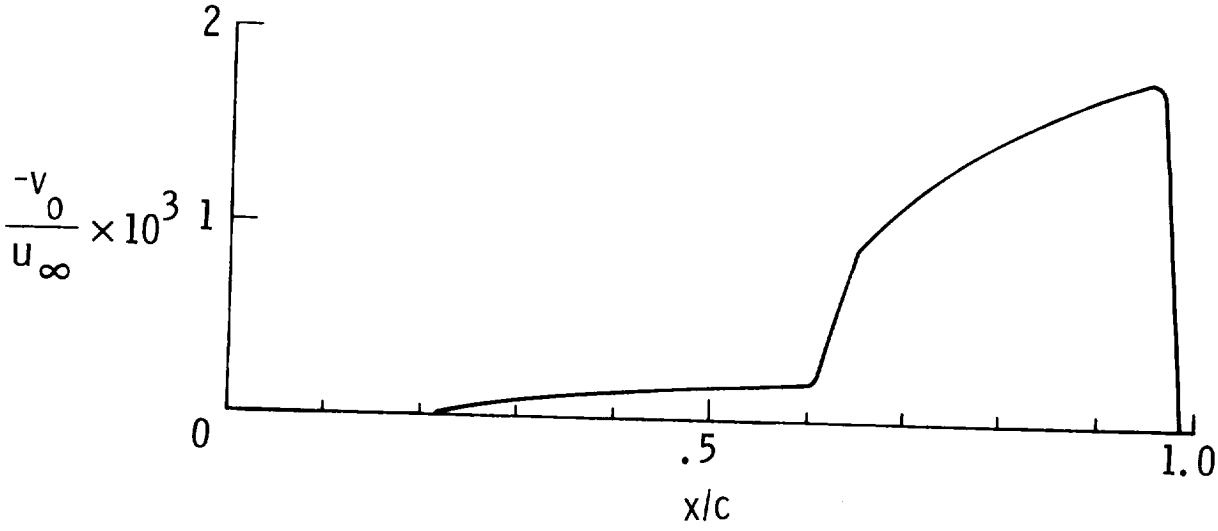

(b) Suction distribution.

Figure 20.- Pressure and suction distributions on Michigan 30° swept wing. u_∞ = 76 m/sec; $R_c = 10.6 \times 10^6$; $\alpha = 0°$.

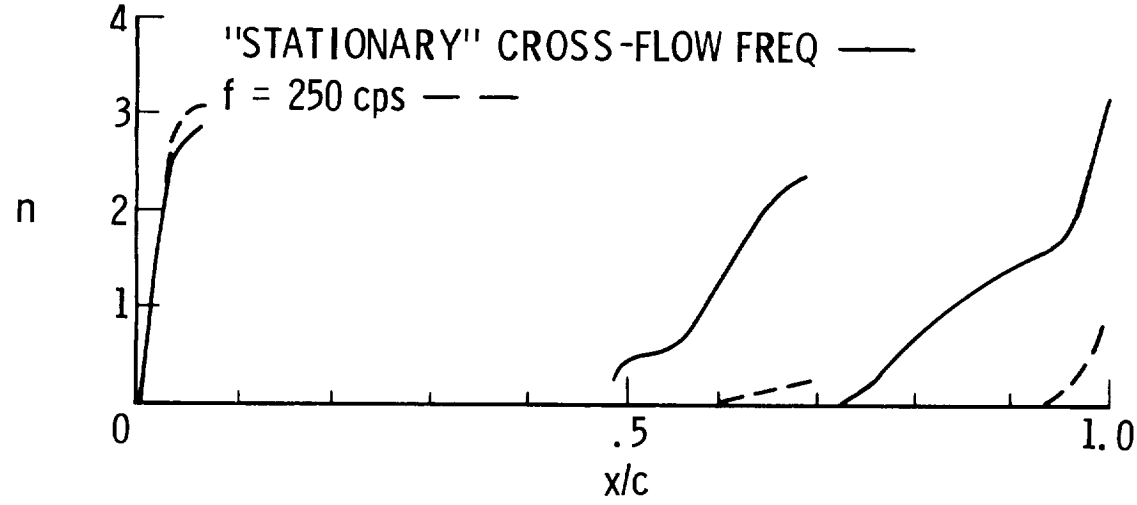

Figure 17.- Integrated amplification ratios on Ames 33° swept wing using envelope method.

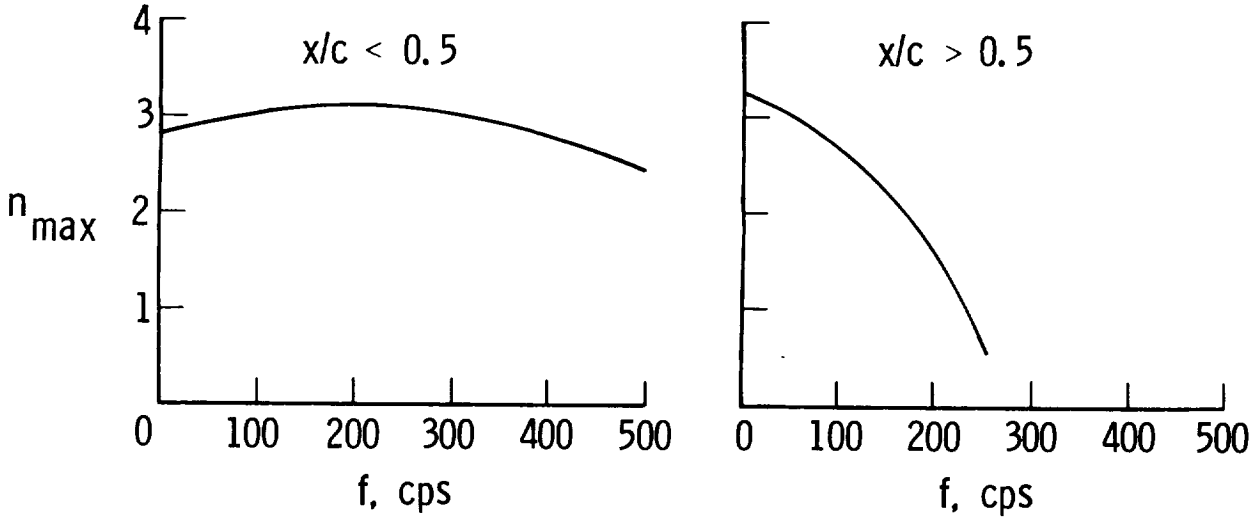

Figure 18.- Maximum integrated amplification ratios on Ames 33° swept wing by envelope method.

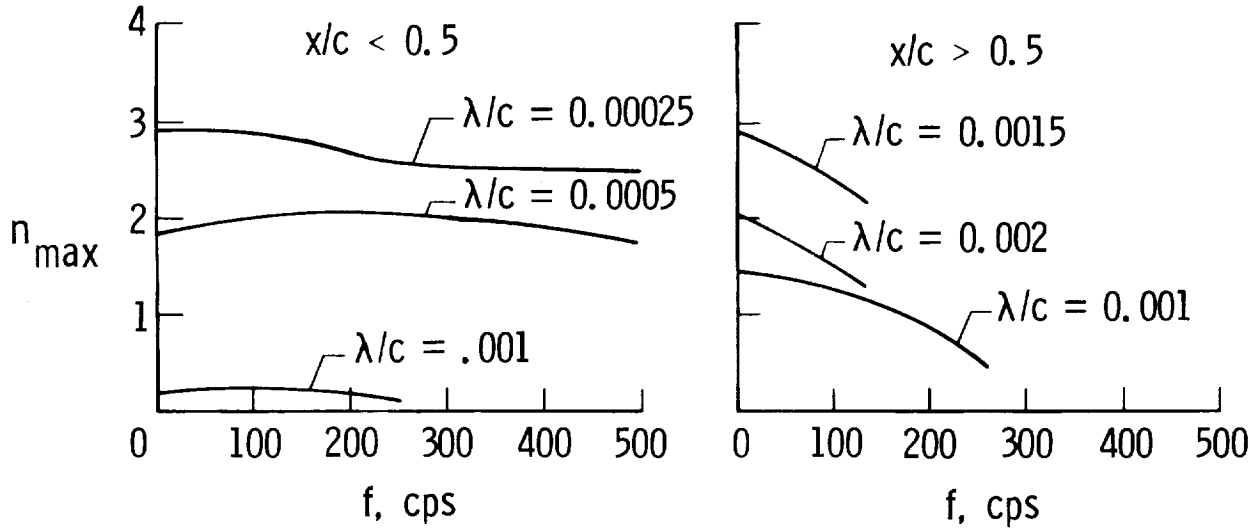

Figure 19.- Maximum integrated amplification ratios on Ames 33° swept wing by fixed wavelength/frequency method.

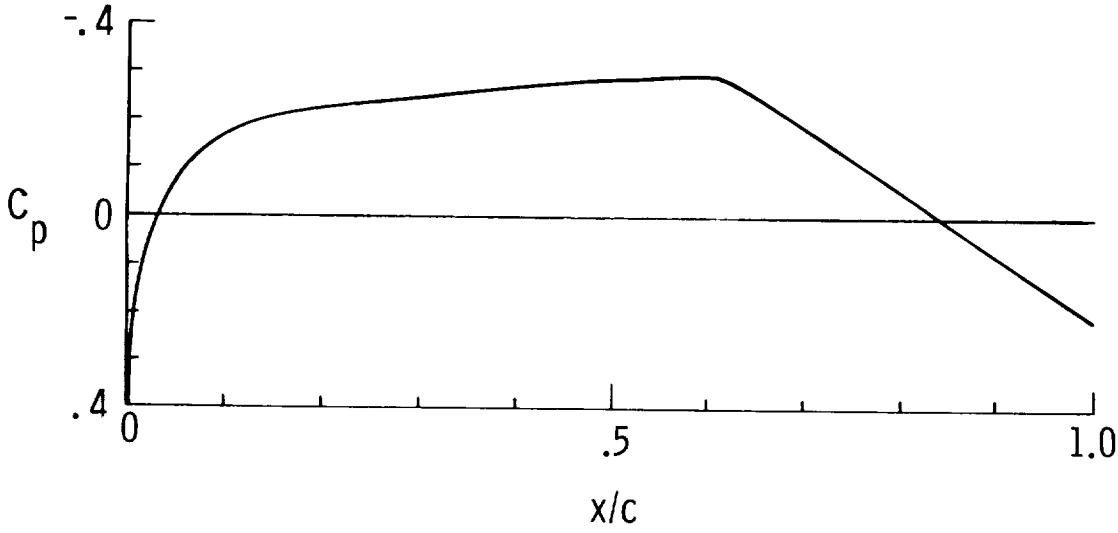

(a) Pressure distribution.

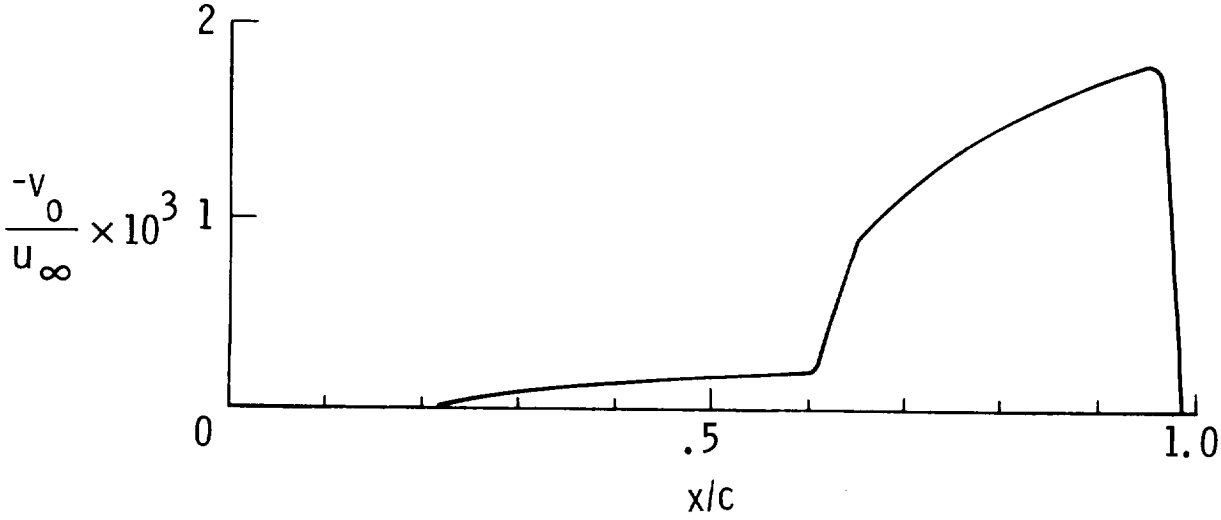

(b) Suction distribution.

Figure 20.- Pressure and suction distributions on Michigan 30° swept wing. u_∞ = 76 m/sec; $R_c = 10.6 \times 10^6$; $\alpha = 0°$.

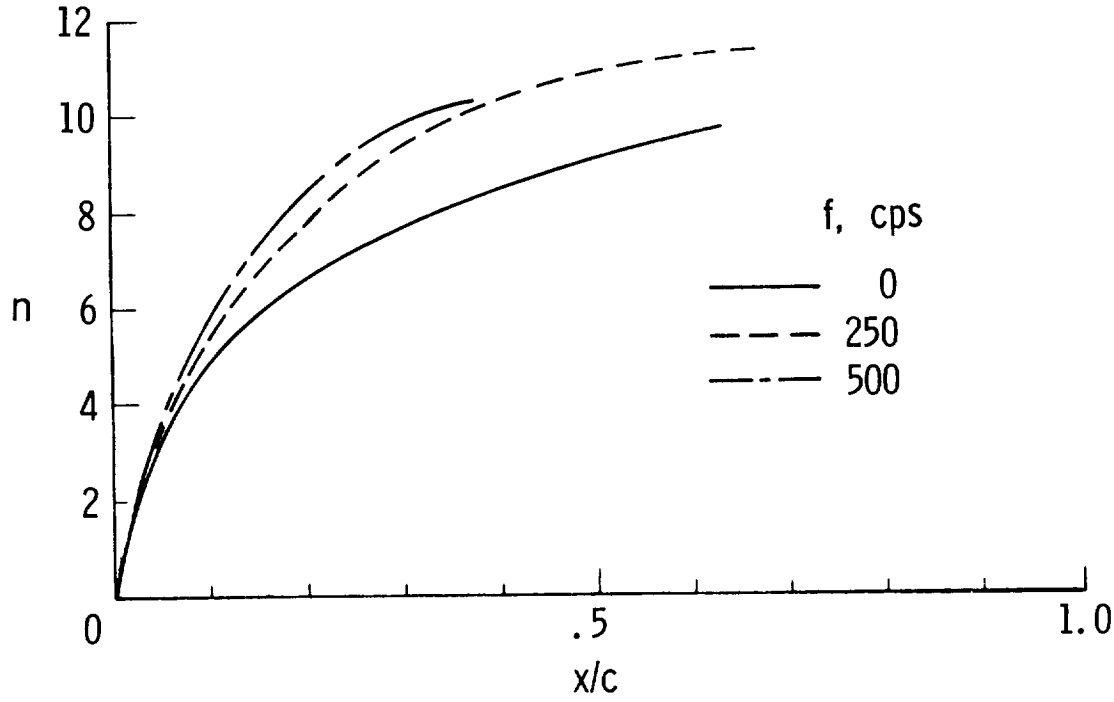

Figure 21.- Integrated amplification ratios on Michigan 30° swept wing using envelope method.

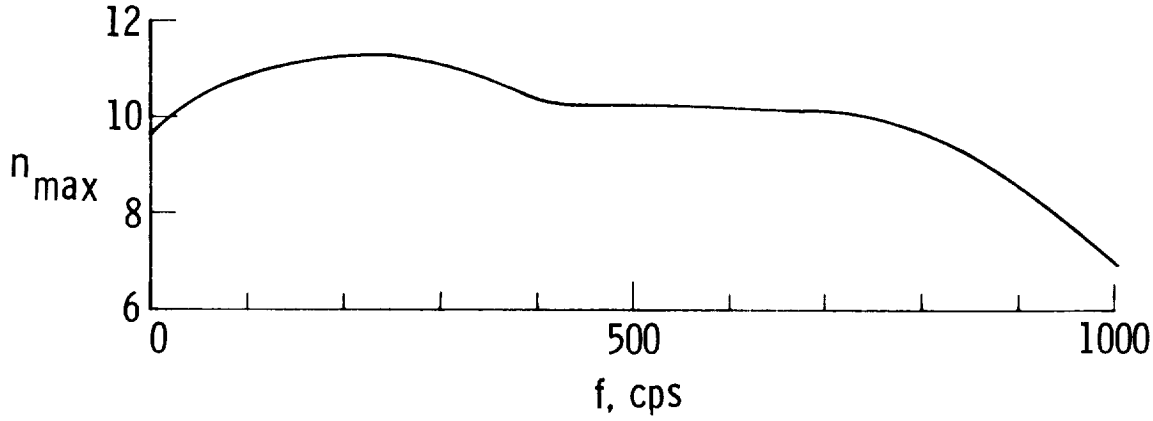

Figure 22.- Maximum integrated amplification ratios on Michigan 30° swept wing by envelope method.

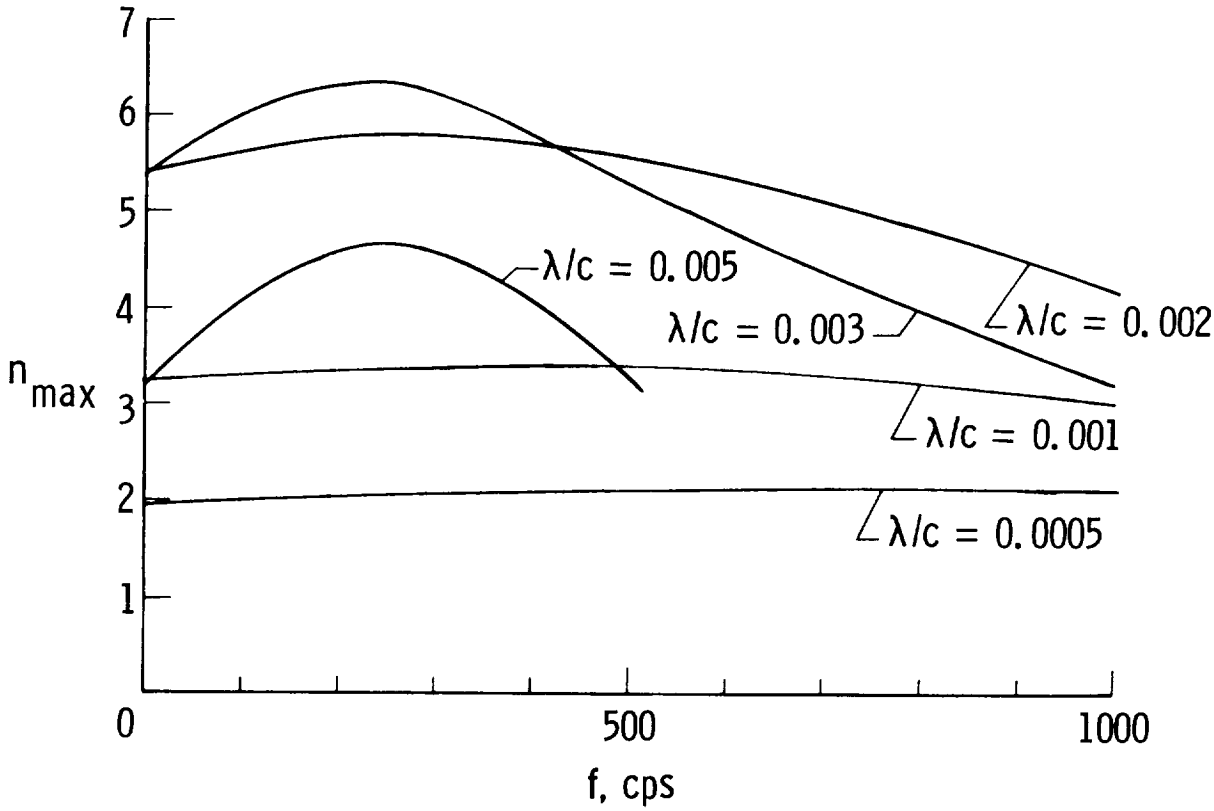

Figure 23.- Maximum integrated amplification ratios on Michigan 30° swept wing by fixed wavelength/frequency method.

1. Report No.	2. Government Accession No.	3. Recipient's Catalog No.
NASA TP-1645		

4. Title and Subtitle	5. Report Date
STATUS OF LINEAR BOUNDARY-LAYER STABILITY THEORY AND THE e^n METHOD, WITH EMPHASIS ON SWEPT-WING APPLICATIONS	April 1980
	6. Performing Organization Code
7. Author(s)	8. Performing Organization Report No.
Jerry N. Hefner and Dennis M. Bushnell	L-13313
	10. Work Unit No.
	505-31-23-03
9. Performing Organization Name and Address	11. Contract or Grant No.
NASA Langley Research Center Hampton, VA 23665	
	13. Type of Report and Period Covered
12. Sponsoring Agency Name and Address	Technical Paper
National Aeronautics and Space Administration Washington, DC 20546	14. Sponsoring Agency Code

15. Supplementary Notes

This paper is an expansion of AIAA Paper 79-1493.

16. Abstract

The state of the art for the application of linear stability theory and the e^n method for transition prediction and laminar-flow-control design are summarized, with new analyses of previously published low-disturbance, swept-wing data presented. The major difficulty was found to be the paucity of detailed information regarding stream and wall disturbances and their receptivity within the boundary layer. For any set of transition data with similar stream disturbance levels and spectra, the e^n method for estimating the beginning of transition worked reasonably well; however, even within a given data set, the value of n could vary significantly, evidently depending upon variations in disturbance field or receptivity. For data where disturbance levels were high, the values of n were appreciably below the usual average value of 9 to 10 obtained for relatively low disturbance levels. It is recommended that the design of laminar-flow-control systems be based on conservative estimates of n and that, in considering the values of n obtained from different analytical approaches or investigations, the designer explore the various assumptions which entered into the analyses.

17. Key Words (Suggested by Author(s))	18. Distribution Statement
Transition prediction e^n method Linear stability theory Laminar flow control Swept wing	Unclassified - Unlimited Subject Category 34

19. Security Classif. (of this report)	20. Security Classif. (of this page)	21. No. of Pages	22. Price*
Unclassified	Unclassified	47	$4.50

* For sale by the National Technical Information Service, Springfield, Virginia 22161

NASA-Langley, 1980